https://doi.org/10.5194/essd-2026-106
Preprint. Discussion started: 26 February 2026
© Author(s) 2026. CC BY 4.0 License.

Open Access Earth System Science Data Discussions

Consolidating Global Estimates of Ocean Heat Content: Toward a Consistent Earth Heat Inventory

Audrey Minière[1], Karina von Schuckmann[2] and Sabrina Speich[1]

[1]Laboratoire de Météorologie Dynamique, 24 rue Lhomond, 75005 Paris, France
[2]Mercator Ocean International, 2 Av. de l'Aérodrome de Montaudran, 31400 Toulouse, France

Correspondence to: Audrey Minière (audrey.miniere@lmd.ipsl.fr)

Abstract. The Earth's Energy Imbalance (EEI), defined as the difference between the incoming solar radiation and the outgoing terrestrial radiation at the top of the atmosphere, provides a fundamental measure of anthropogenic climate change. Today, this imbalance is positive, indicating that the Earth system is accumulating heat, of which more than 90% is stored in the ocean. The evolution of Global Ocean Heat Content (GOHC) thus constitutes a critical indicator of planetary warming and underpins the Earth Heat Inventory, currently the only approach capable of quantifying the observed absolute value of the EEI. Yet, the lack of standardized calculation protocols and the diversity of methodological choices across studies hinder the comparability of GOHC estimates and obscure the traceability of associated uncertainties. Here, we present a comprehensive, transparent assessment of GOHC trends and uncertainties based on an ensemble of 13 gridded in situ ocean temperature products spanning 1960–2024. Building on prior community efforts, we systematically evaluate the sensitivity of GOHC trends to key methodological choices, including (i) the temperature product, (ii) the definition of the temperature variable, (iii) the treatment of seawater density and heat capacity, (iv) the ocean domain used for integration, and (v) the method used for trend estimation. Our results demonstrate that GOHC trends are remarkably robust across methodological configurations. Variations associated with the temperature variable definition, thermodynamic parameters, ocean domain, or trend estimation method remain below 0.1 W m^{-2}, well within the ensemble-mean uncertainty range of 0.21 W m^{-2}, across both recent decades and multi-decadal timescales. We further show that the substantial spread among published EEI estimates reflects pronounced temporal variability in ocean heat uptake rates. This variability renders EEI estimates highly sensitive to the selected averaging period, underscoring that present-day absolute EEI values can only be meaningfully interpreted in a long-term context. We demonstrate that the ensemble spread provides a practical and comprehensive proxy for GOHC uncertainty, consistent with product-specific uncertainty estimates. By consolidating international assessment practices, this study delivers a transparent characterization of the state of ocean warming and provides a fully documented, openly available framework for constructing a GOHC indicator. Together, these advances strengthen the Earth Heat Inventory estimate, establish a reliable benchmark for monitoring ocean warming and EEI, facilitate intercomparison across studies, and reinforce international climate assessments at the science and policy interface.

https://doi.org/10.5194/essd-2026-106
Preprint. Discussion started: 26 February 2026
© Author(s) 2026. CC BY 4.0 License.

Open Access Earth System Science Data Discussions

1 Introduction

The ocean is currently warming at an unprecedented rate since at least the 1950s (Cheng et al., 2022a; IPCC, 2021). This continuous warming, extending from the surface to the abyss, is a clear manifestation of the persistent anthropogenic Earth's Energy Imbalance (EEI) at the top of the atmosphere (Loeb et al., 2021; von Schuckmann et al., 2023). This imbalance is primarily driven by human-induced CO_2 emissions, which traps excess heat within the Earth system, resulting in incoming energy flux exceeding outgoing radiation at the top of the atmosphere (Hansen et al., 2005). Absorbing over 90% of this excess energy, the ocean serves as both an archive of Earth's heating and an Earth's system climate regulator (von Schuckmann et al., 2023).

The evolution of global ocean heat content (GOHC) provides information about the magnitude and variability of EEI, making it a critical indicator for monitoring past, current and future climate change. Observational records show that GOHC has increased continuously since the mid-20th century, with the past decade alone setting successive annual records (Cheng et al., 2025; Pan et al., 2025), alongside a about twofold increase in the rate of ocean warming over the last two decades (Forster et al., 2024; Pörtner et al., 2019; von Schuckmann et al., 2023). This finding underscores an alarming reality: ocean warming is not only ongoing, it has been accelerating for the past 60 years (Minière et al., 2023; Storto and Yang, 2024). The impacts of such warming are numerous, severe, and already affecting both marine ecosystems and human societies (Cheng et al., 2022c; Gulev et al., 2021).

Global Mean Surface Temperature (GMST) is a widely used benchmark of global warming (IPCC, 2022). However, as the indicator of GMST is highly sensitive to natural variability, it makes it difficult to detect key temperature thresholds in real time, such as the 1.5°C limit set by the Paris Agreement (Betts et al., 2023). Using the global climate indicator of the rate of change in GOHC provides an integrated view of energy accumulation throughout the full depth of the ocean. This makes it a complementary robust indicator for detecting long-term climate trends (von Schuckmann et al., 2016), including the emergence of critical warming thresholds (Merchant et al., 2025; Minobe et al., 2025; Rockström et al., 2024).

Yet, despite the central role of this global climate indicator, no standardized protocol currently exists for estimating GOHC. Variations in data sources, methodological choices, and post-processing procedures lead to discrepancies across studies, limiting comparability and confidence in estimated ocean warming rates and EEI. Figure 1 presents a synthesis of a wide range of published estimates of global warming. Most of these represent trends in the Earth's Heat Inventory (von Schuckmann et al., 2020, 2023), which accounts for heat stored across the ocean, cryosphere, continents, and atmosphere. Given the ocean's dominant role as a heat reservoir, most estimates specifically pertain to OHC, which can be calculated using both direct and indirect approaches. The direct method relies on gridded *in situ* subsurface temperature products (Cheng et al., 2017; Ishii et al., 2017; Levitus et al., 2012). In contrast, indirect methods infer OHC through alternative observation-based approaches. These include ocean reanalyses that assimilate various observations streams into models (Balmaseda et al., 2013; Lellouche et al., 2021; Storto and Yang, 2024), as well as sea-level budget approaches that estimate OHC from satellite altimetry and gravimetry (Hakuba et al., 2021, 2024; Marti et al., 2022, 2024). Additional indirect approaches leverage atmospheric oxygen measurements (Resplandy et al., 2019), sea surface temperature

https://doi.org/10.5194/essd-2026-106
Preprint. Discussion started: 26 February 2026
© Author(s) 2026. CC BY 4.0 License.

advection reconstructions using Green's functions (Wu et al., 2025; Zanna et al., 2019) or machine learning techniques such as neural networks (Bagnell and DeVries, 2021; Su et al., 2021, 2023). On paleoclimatic timescales, atmospheric proxies are used to reconstruct OHC (Baggenstos et al., 2019; Shackleton et al., 2023, 2025). Some studies also use satellite-derived estimates of the global net radiative flux at the top of the atmosphere (e.g., the Clouds and the Earth's Radiant Energy System project, CERES; Loeb et al., 2021), while others rely on climate model outputs based on radiative fluxes or heat content trends (e.g., Cuesta-Valero et al., 2021; Smith et al., 2015; Wild, 2020).

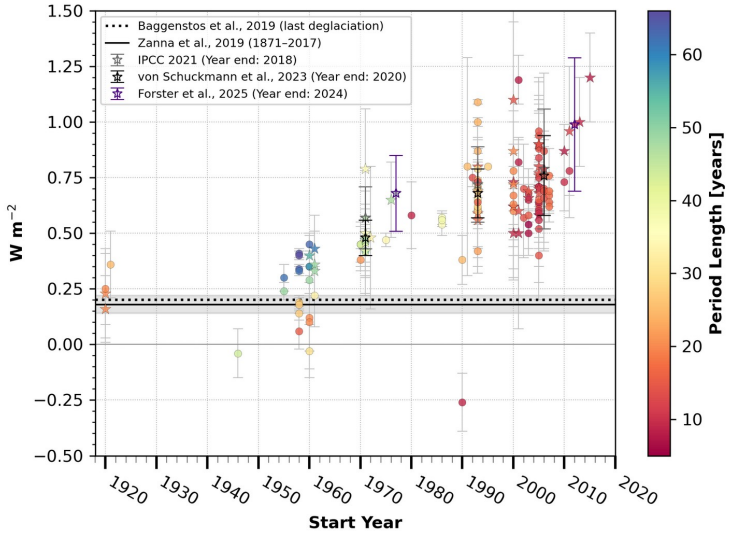

Figure 1 | Literature assessment of Earth's Energy Imbalance. Each estimate is derived from a published study (see) and converted, where necessary, to comparable units of W m^{-2} relative to the Earth's surface. Ocean warming estimates are shown by the circles, while total planetary warming estimates (i.e., EEI) are represented by stars. Figure updated from Minière et al. (2023). See Fig. S1 and *Code and Data Availability* section for a comprehensive overview of methods and references.

In this analysis, we focus exclusively on estimates of ocean warming derived from *in situ* observations of subsurface ocean temperature. As international efforts to track and respond to climate change intensify, including within the frameworks of the Intergovernemental Panel on Climate Change (IPCC, https://www.ipcc.ch/), the Global Climate Observing System (GCOS, https://gcos.wmo.int/), and the World Meteorological Organization (WMO, https://public.wmo.int/en), the need for a scientifically rigorous and harmonized framework (Betts et al., 2023) such as for GOHC estimates has become increasingly urgent. A reliable indicator of ocean warming is essential not only for understanding past and ongoing climate change, but also for advancing climate science, informing decision-making, guiding climate reporting, and supporting global stocktaking efforts. Motivated by this need, our study develops a comprehensive methodology designed to enable consistent and scientifically robust assessments of ocean heat content. Our approach is grounded in the integration of multiple observational datasets and a systematic evaluation of methodological sensitivities. By establishing transparent guidelines, our goal is to facilitate the production of reproducible, reliable and policy-relevant GOHC estimates, thereby reinforcing the foundations of global climate monitoring.

https://doi.org/10.5194/essd-2026-106
Preprint. Discussion started: 26 February 2026
© Author(s) 2026. CC BY 4.0 License.

The paper is structured as follows. In Section 1, we review and quantify the current state of knowledge on ocean warming, comparing published estimates with our calculations. Section 2 presents and details the methodological approach employed in this study, including the treatment of in situ gridded temperature products and sensitivity analyses. Finally, in Section 3, we discuss the results and provide recommendations for enhancing the robustness and transparency of global ocean heat content estimates.

2 How fast is the ocean warming?

A broad range of published estimates of the EEI, including the most recent literature, is synthesized and updated from Minière et al. (2023), as illustrated in Fig. 1. On decadal to multidecadal timescales, studies show that global heating rates since the 1960s range between 0.2 and 1 W m^{-2}. Yet, even in the 21st century, when observational coverage and data quality improved substantially (Abraham et al., 2013; Meyssignac et al., 2019; Cheng, et al., 2022), the spread among estimates remains large (~0.5–1 W m^{-2}).

Despite this spread, a consistent picture emerges across independent estimation methods (in situ observations, reanalyses, satellite-derived estimates, and paleoclimate reconstructions; see Fig. S1): (i) the EEI has remained positive for at least the past six decades; (ii) the magnitude of EEI has increased in recent decades, reflecting the acceleration of excess heat accumulation within the Earth system (Minière et al., 2023). On longer timescales, Zanna et al. (2019) reported an imbalance of 0.18 ± 0.04 W m^{-2} since 1870, while paleoclimate proxies suggest a persistent imbalance of ~0.2 W m^{-2} during the last deglaciation (~10,000 years; Baggenstos et al., 2019). Since 1960, decadal mean values have consistently exceeded these long-term reconstruction and paleo-based reference levels. Since 1990, decadal heating rates have risen to more than doubled relative to those of the deglaciation, underscoring the unprecedented pace of contemporary ocean warming. Although outliers exist (e.g., a negative decadal estimate starting in 1990; Balmaseda et al., 2013), the overall evidence indicates that EEI has continued to increase toward the present.

Focusing on the ocean, Fig. 2 shows both the cumulative ocean heat inventory since 1960 (panel a) and the corresponding 15-year GOHC running trends (panel b). Between 1960 and 2024, the upper 2000 m of the ocean stored a total of 334 ± 25 ZJ of heat. The vertical distribution was 45 ± 4% (149 ± 16 ZJ) in the 0–300 m layer, 23 ± 3% (77 ± 11 ZJ) in the 300–700 m layer, and 32 ± 3% (107 ± 8 ZJ) in the 700–2000 m layer. Over the more recent period 2005–2024, the ocean gained 185 ± 21 ZJ within the 0–2000 m layer, with similar relative contributions across depth ranges. These values are broadly consistent with Pan et al. (2025), who reported, for 1960–2024, that 42% of the accumulated heat was stored in the 0–300 m layer, 22% in the 300–700 m layer, and 29% in the 700–2000 m layer.

When expressed as heating rates per unit of Earth's surface area, ocean warming rates exhibit a clear increase between the long-term and recent periods (Table 1). The mean ocean heating rate rose from 0.32 ± 0.02 W m^{-2} over 1960–2024 to 0.60 ± 0.07 W m^{-2} over 2005–2024. This increase is evident across all ocean layers (Table 1) and aligns with previously reported trends (e.g., von Schuckmann et al., 2023), reflecting the ongoing acceleration of ocean heat accumulation (Minière et al., 2023).

https://doi.org/10.5194/essd-2026-106
Preprint. Discussion started: 26 February 2026
© Author(s) 2026. CC BY 4.0 License.

Ocean layer (m)	1960–2024 (W m^{-2})	1960–2020 (W m^{-2}) von Schuckmann et al., 2023	2005–2024 (W m^{-2})	2006–2020 (W m^{-2}) von Schuckmann et al., 2023
0-300	0.14 ± 0.01	0.14 ± 0.04	0.27 ± 0.03	0.27 ± 0.10
0-700	0.22 ± 0.02	0.21 ± 0.10	0.39 ± 0.05	0.39 ± 0.10
700-2000	0.10 ± 0.01	0.11 ± 0.04	0.20 ± 0.03	0.23 ± 0.10
0-2000	0.32 ± 0.02	0.32 ± 0.10	0.60 ± 0.07	0.62 ± 0.20

Table 1 | Global ocean heat content rates. Heating rates are expressed in W m^{-2} relative to the Earth's surface area, for different depth layers and time periods. Rates were computed using the LOWESS method (see Section 3.2) to allow direct comparison with the estimates of von Schuckmann et al. (2023). Estimates for 1960–2024 and 2005–2024 are computed from this study GOHC ensemble mean, while values for 1960–2020 and 2006–2020 are taken from von Schuckmann et al. (2023).

As highlighted by Minière et al. (2023) for decadal heating rates, the 15-year ocean heating rates exhibit pronounced multidecadal variability prior to the 2000s, with notable phases of rapid increase during the 1960s–1970s and 1980s–1990s (Fig. 2b). Specifically, ocean heating rates rose by 0.31 ± 0.50 W m^{-2} between 1960–1974 and 1967-1981, and by 0.56 ± 0.32 W m^{-2} between 1976–1990 and 1993–2007. Over the longer term, the 15-year heating rates increased by 0.66 ± 0.43 W m^{-2} between 1960–1974 and 2010–2024, indicating a sustained acceleration in ocean heat uptake. This variability seems to be largely driven by the upper 0–300 m layer, while deeper layers (700-2000 m and 300–2000 m) show more moderate fluctuations (Fig. 2b). Nonetheless, the long-term upward trend is evident across all layers, with the most recent two decades' increase largely captured by the 0–300 m layer, highlighting the dominant role of the upper ocean in recent ocean warming.

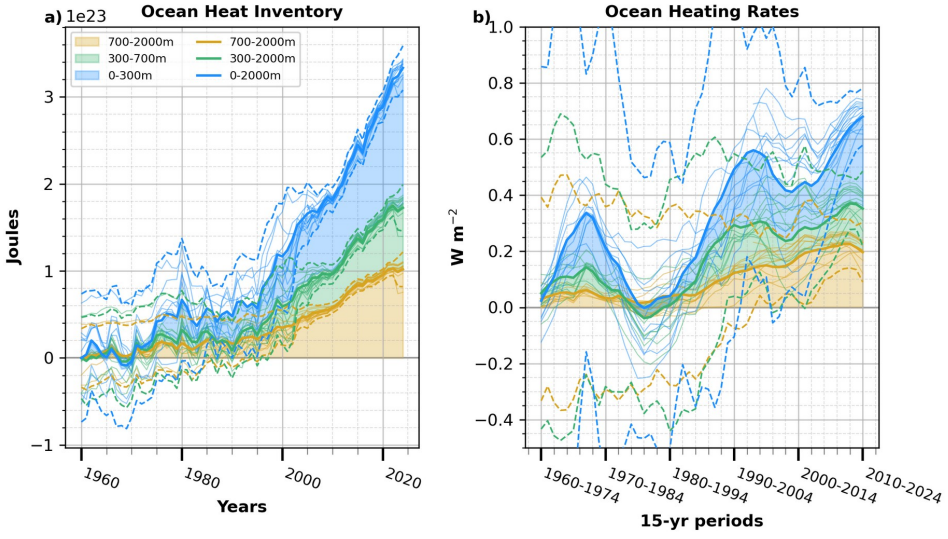

Figure 2 | Ocean heat inventory and heating rates. (a) Global Ocean Heat Content (GOHC) for the 700–2000 m (yellow), 300–2000 m (green), and 0–2000 m (blue) layers, based on an ensemble of in situ temperature products (see Table 2). Thin lines represent individual products, bold lines the ensemble mean, and dashed lines

https://doi.org/10.5194/essd-2026-106
Preprint. Discussion started: 26 February 2026
© Author(s) 2026. CC BY 4.0 License.

twice the ensemble spread. A surface ocean mask was applied, excluding areas shallower than 300 m and latitudes beyond 60°. **(b)** Fifteen-year running ocean heating rates derived from ordinary least squares regression of the ensemble mean GOHC (bold lines). Dashed lines show the 95% confidence intervals accounting for autocorrelation and computed based on a weighted least squares regression, and thin lines show heating rates from individual products.

Beyond OHC alone, these results provide, for the first time, a depth-resolved perspective on the EEI, made possible by subsurface temperature observations. The analysis reveals that variability in EEI is coherent across depth layers, with different depth ranges tending to warm simultaneously but with varying amplitudes. This finding highlights that EEI is best assessed over long timescales, i.e., multidecadal periods and longer, since shorter-term estimates (i.e., on interannual or decadal timescales) are strongly affected by decadal to multidecadal variability as well as observational uncertainties. Importantly, the spread among published EEI estimates shown in Fig. 1 cannot be attributed solely to methodological differences; a substantial part also arises from the intrinsic temporal variability of EEI, which makes estimates highly sensitive to the chosen averaging period. Consequently, short-term values (whether monthly, annual, or even decadal) must be interpreted within a longer-term context to determine whether they reflect phases of rapid increase, relative slowdown, or quasi-stability. Present-day EEI estimates can therefore only be meaningfully assessed when viewed in this broader temporal framework. Further work is needed to better understand the origins of variability in ocean heating rates and EEI, and to quantify the respective contributions of externally forced trends and internal climate variability.

Nevertheless, significant uncertainties remain (Fig. 2b). While the ensemble mean captures the overarching signal, individual products differ in the magnitude and phasing of their temporal variability. Some datasets exhibit stronger fluctuations than others, even though all remain within the ensemble uncertainty envelope. These discrepancies illustrate the sensitivity of GOHC estimates to methodological choices made at each step of the calculation. In this sense, the GOHC indicator encapsulates a considerable degree of complexity, from the acquisition of raw temperature measurements to the derivation of the final ocean heat content estimate. Each methodological choice, whether in the selection of the observational product, the integration of seawater temperature over the ocean volume, the choice of the temporal window and regression method for trend estimation, or the treatment of uncertainties, can influence the resulting GOHC trends and contribute to the spread seen in Fig. 1 and the ensemble variance in Fig. 2. Put differently, the question *"How fast is the ocean warming?"* cannot be answered independently of *"How do we estimate it?"*. This consideration motivates the next section, where we present our methodology for deriving GOHC from in situ temperature products, evaluate the sensitivity of the results to key methodological assumptions, and discuss the associated uncertainties.

3 How to estimate the GOHC indicator ?

When estimating GOHC, methodological choices can be broadly classified into two categories: *pre-processing* choices and *post-processing* choices, both related to the gridded temperature product and defined as follows. Pre-processing encompasses all steps undertaken before the production of a gridded temperature product, including instrumental bias corrections (e.g., Cheng et al., 2014; Gouretski and Cheng, 2020) quality control (QC) procedures (Tan et al., 2022, 2023; Zhang et al., 2024), spatial and temporal interpolation methods (often referred to as mapping, Cheng et al., 2015; Li et al., 2022; Lyman and Johnson, 2008), the choice of first-guess

https://doi.org/10.5194/essd-2026-106
Preprint. Discussion started: 26 February 2026
© Author(s) 2026. CC BY 4.0 License.

fields to fill data gaps, and the reference climatology used to define anomalies (Cheng and Zhu, 2015; Lyman and Johnson, 2014). Post-processing, by contrast, refers to the methodological decisions applied after gridded fields have been generated particularly in the computation of GOHC and its derived quantities such as anomalies, trends (Cheng et al., 2022b), or acceleration rates (Minière et al., 2023). These successive processing steps, and the associated propagation of uncertainties, are illustrated in Fig. 3, which highlights how methodological decisions taken from raw observations to the final GOHC time series influence both absolute values and temporal changes. In the absence of standardized guidelines, these steps are implemented differently across research groups, potentially limiting comparability and introducing biases or artifacts. This underscores the need for a systematic evaluation of each step to establish best-practice recommendations and advance toward a harmonized framework. Such coordinated efforts would reduce uncertainties in GOHC estimates while enhancing their robustness, reproducibility, and policy relevance.

While the sensitivity of GOHC estimates to pre-processing steps has been extensively documented (e.g., Boyer et al., 2016; Savita et al., 2022), our analysis shifts the focus toward post-processing steps. We begin by outlining the theoretical basis for deriving GOHC from gridded subsurface temperature products. Beyond the time series itself, the key quantity for climate monitoring is the rate of excess energy accumulation in the ocean, expressed in W m^{-2}, which can be directly compared to the EEI. We then investigate how methodological assumptions and variable definitions influence the estimation of GOHC trends from gridded subsurface temperature fields. Specifically, we assess five key factors: (i) the choice of gridded temperature product, (ii) the definition of the temperature variable, (iii) the treatment of seawater density and heat capacity (constant vs. variable), (iv) the integration domain, and (v) the method used for trend estimation. Finally, we present the results of these sensitivity tests and conclude the section with a discussion on the quantification of uncertainties in GOHC estimates.

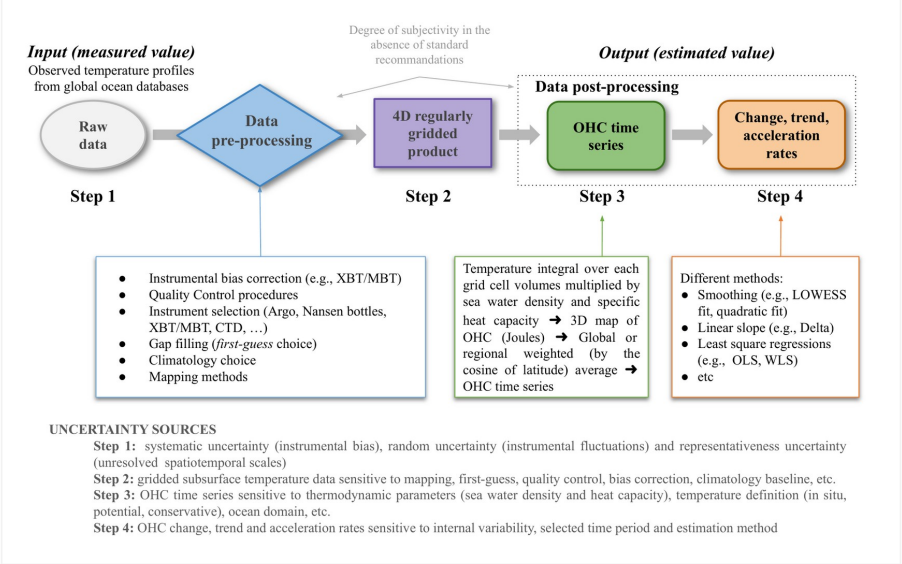

Figure 3 | Diagram illustrating the processing steps involved in the GOHC estimation, and the traceability of uncertainties from in situ temperature measurements to the estimation of GOHC and its derived quantities.

https://doi.org/10.5194/essd-2026-106
Preprint. Discussion started: 26 February 2026
© Author(s) 2026. CC BY 4.0 License.

3.1 From subsurface temperature to global OHC: theoretical framework and definitions

The ocean heat balance can be expressed as follows (Ma et al., 2020):

$$OHS = OHU - \nabla_h(OHT) + Diff \quad (2.1)$$

where OHS denotes the ocean heat storage at a given location, which is governed by three terms: the ocean heat uptake (OHU), the horizontal divergence (∇_h) of ocean heat transport (OHT), and heat changes associated with diffusion processes (Diff). OHC is expressed in Joules (J) or Joules per square meter (J m^{-2}), while OHU and OHS are typically reported in Watts per square meter (W m^{-2}). At the global scale, the transport and diffusion terms cancel out, such that OHU can be approximated by OHS. Consequently, ocean heat storage is equivalent to the net heat fluxes at the air-sea interface. As a result, the terms *OHU*, *OHS*, and *OHC tendency* are often used interchangeably at the global level, although their definitions may differ between studies. For example, OHS is sometimes used to denote the ocean heat content anomaly (e.g., (Cheng et al., 2022b), while in other contexts, it refers specifically to the OHC tendency (e.g., Ma et al., 2020; Meyssignac et al., 2019).

OHC represents the amount of thermal energy stored in the ocean. Its computation is based on the vertical integration of ocean temperature over the ocean volume. For a given oceanic grid cell located at coordinates (x, y), the local ocean heat content OHC(t,x,y) at time t is defined as:

$$OHC(t,x,y) = A(x,y)\sum_z \rho(t,x,y,z)C_p(t,x,y,z)T(t,x,y,z)h(x,y,z) \quad (2.2)$$

where T is the ocean subsurface temperature (°C), ρ is the seawater density (kg m^{-3}), Cp is the specific heat capacity of seawater (J kg^{-1} $°C^{-1}$), $A(x,y)$ is the area (in m^2) of the grid cell at longitude x and latitude y, and $h(x,y,z)$ is the thickness (m) of the layer at depth z of within the grid cell (x, y). The area of each grid cell is computed as a function of its latitude, so that grid cells at higher latitudes (covering smaller surface areas than those near the equator) are appropriately weighted.

At regional or global scales, the time series of ocean heat content OHC(t) is obtained by summing the local value over the ocean surface:

$$OHC(t) = \sum_{x,y} OHC(t,x,y) \quad (2.3)$$

At the global scale, this time series is referred to as GOHC. In practice, GOHC is almost always considered in terms of anomalies rather than absolute values, primarily due to uncertainties in reference climatologies and the difficulty of defining a consistent, long-term baseline (Cheng and Zhu, 2015, see Fig. S2). The emphasis therefore lies on changes in GOHC relative to a reference period (i.e., an *anomaly*), especially the heat gain or the rate of warming, rather than on the absolute amount of energy stored in the system.

https://doi.org/10.5194/essd-2026-106
Preprint. Discussion started: 26 February 2026
© Author(s) 2026. CC BY 4.0 License.

To enable intercomparison among different estimates of ocean heat content derived from various temperature products, OHC anomalies must be computed relative to a common reference period shared by all datasets. In climate data analysis (see for example Thomson and Emery, 2014), several approaches are commonly used to align time series to a common temporal baseline. One basic method consists in subtracting, from each time series, its mean value over a chosen reference period thereby centering the series around zero for that interval. For monthly data, it is also useful to remove the seasonal cycle to isolate interannual to decadal variability. This can be achieved by applying smoothing methods (annual means, running means, low-pass filters), by subtracting the mean seasonal cycle, or by using spectral filtering (e.g., Fourier decomposition) to remove the dominant harmonics such as the annual and semi-annual components. In this analysis of OHC time series, we compute the mean seasonal cycle of OHC over a specified reference period, denoted as OHC_{clim}, defined as follows:

$$OHC_{clim}(m)=\frac{1}{N}\sum_{i=1}^{N} OHC(m_i)\,, \quad (2.4)$$

where $OHC_{clim}(m)$ is the average value of global or regional OHC for month m, N is the number of available years, and $OHC(m_i)$ is the OHC value for month m in year i. The OHC anomaly is then calculated as the difference between the monthly OHC value and its corresponding monthly climatological mean as follow:

$$OHCA(t)=OHC(t)-OHC_{clim}(t_m)\,, \quad (2.5)$$

where the index m corresponds to the month associated with date t. At the global scale, this anomaly time series is referred to as GOHCA.

Having established the theoretical framework for deriving GOHC from subsurface temperature fields, we next assess how methodological choices influence these estimates. The following sensitivity analysis explores how different assumptions and processing steps affect the robustness of GOHC trends.

3.2 Framework of the sensitivity analysis

3.2.1 Temperature product sensitivity

Various gridded in situ temperature products are available, each applying distinct methodological approaches to interpolate irregularly distributed profiles onto regular spatiotemporal grids in longitude, latitude, depth, and time (Abraham et al., 2013; Boyer et al., 2016; Liang et al., 2021; Savita et al., 2022). In this study, we compute GOHC using an ensemble mean approach, comparing individual estimates against both the ensemble mean and its spread (standard deviation). The products, their abbreviations and references are listed in Table 2.

Most datasets are produced using objective analysis, a statistical framework that minimizes a predefined error function while accounting for spatial and temporal correlations (Stammer et al., 2021). Within this framework, ISAS, CORA5.2, ARMOR3D, EN4, MOAA, and SIO employ different correlation radii and error functions; BOA uses a successive Barnes scheme; Ishii and NCEI apply group-weighted averaging; and IAP relies on an initial CMIP5-based climatology further refined through error covariance estimates (Cheng and Zhu, 2016). In

https://doi.org/10.5194/essd-2026-106
Preprint. Discussion started: 26 February 2026
© Author(s) 2026. CC BY 4.0 License.

283 contrast, the RFROM dataset is derived from a machine learning model trained to reproduce vertically
284 integrated OHC anomalies using predictors such as sea surface height (SSH), sea surface temperature (SST),
285 time, latitude, and longitude.

286 The products also differ in their underlying data sources. Several (e.g., MOAA GVP, NCEI, EN4, IAP, ISHII,
287 CORA5.2, RFROM) integrate a wide range of historical and modern observations, including Mechanical and
288 Expendable Bathythermographs (MBT, XBT), Conductivity–Temperature–Depth (CTD) measurements, and
289 Argo profiles. ARMOR3D and RFROM additionally assimilate satellite altimetry. Products such as IPRC,
290 ISAS, GDCSM, BOA, and SIO are based exclusively on Argo observations, restricting their temporal coverage
291 to the modern observing era (2005–present) but ensuring the highest reliability due to the exceptional quantity,
292 quality and continuity of observations during this 'golden period' of the global ocean observing system.
293 Products combining multiple observation types extend further back, to the altimetry era (1993–present) or even
294 to the historical record (1960–present). For the NOAA product, the 0–2000 m monthly estimates were extended
295 prior to 2006 using pentadal NOAA data (Levitus et al., 2012), thereby providing a longer-term record. Despite
296 differences in temporal and depth coverage, all datasets provide estimates down to 2000 m.

297 These reconstructions consistently show significant warming of the upper 2000 m of the ocean over recent
298 decades (see Fig. S3), in agreement with earlier studies (Abraham et al., 2013; Cheng et al., 2022c; Gulev et al.,
299 2021; Levitus et al., 2012). However, discrepancies persist in interannual variability and in estimated warming
300 rates, reflecting differences in mapping methods, XBT bias corrections, and the reference climatologies used to
301 fill data gaps (Boyer et al., 2016; Cheng et al., 2014; Cheng and Zhu, 2015; Lyman et al., 2010). More recent
302 work has highlighted additional sensitivities to the definition of the integration domain (Savita et al., 2022)and
303 to reference climatologies in data-sparse regions (Liang et al., 2021; Lyman and Johnson, 2014).

304 Finally, in constructing the ensemble mean for this study, we consider 13 gridded temperature products. To
305 avoid over-representing the EN4 family, the four EN4 variants (which differ in their XBT bias corrections) are
306 first averaged into a single representative estimate for the ensemble mean, while all four versions are retained
307 when calculating the ensemble spread. This approach prevents bias from a single product family, while ensuring
308 that the ensemble spread fully reflects uncertainties associated with alternative XBT correction schemes. In this
309 analysis, the ensemble spread serves as a practical proxy for GOHC uncertainty.

Product name/ Provider or Institution	Instrument type	T° type (unit)	Salinity type (unit)	Spatial and temporal coverage	Mapping	Reference and Data access link
IPRC	Argo	Potential (°C)	PSU	89°N-89°S (1°x1°), 0-2000m (27 levels), **01/2005 - 04/2020** (monthly)	Variational Interpolation	http://apdrc.soest.hawaii.edu/projects/Argo/data/gridded/On_standard_levels/index-1.html
ISAS/ IFREMER	Argo	Not mentioned (°C)	PSS-78	90°N-77°S (0.12°x0.5°), 1-5500m (187 levels), **01/2002 - 12/2020** (monthly)	Optimal Interpolation	Gaillard et al., 2016; Kolodziejczyk et al., 2021 https://www.seanoe.org/data/00412/52367/
GDCSM/ SHOU	Argo	Not mentioned (°C)	PSS-78	90°N-90°S (1°x1°), 0-1945m (58 levels), **01/2004 - 06/2024** (monthly)	Optimal Interpolation	Zhang et al., 2022 ftp://data.argo.org.cn/pub/ARGO/GDCSM/NETCDF/

https://doi.org/10.5194/essd-2026-106
Preprint. Discussion started: 26 February 2026
© Author(s) 2026. CC BY 4.0 License.

BOA/CSIO/ MNR	Argo	Not mentioned (°C)	PSS-78	80°N-80°S (1°x1°), 0-1945m (58 levels), **01/2004 - 09/2024** (monthly)	Objective Analysis (Barnes successive method)	Li et al., 2017 ftp://data.argo.org.cn/pub/ARGO/BOA_Argo/
SIO/ SCRIPPS	Argo	Potential (°C)	PSS-78	80°N-64°S (1°x1°), 0-1945m (58 levels), **01/2004 - 12/2024** (monthly)	Weighted Least Squares adjustment	Roemmich and Gilson, 2009 https://sio-argo.ucsd.edu/RG_Climatology.html
MOAA GPV/ JAMSTEC	Argo + others	Potential (°C)	PSS-78	70°N-60°S (1°x1°), 10-1971m (25 levels), **01/2001 - 05/2024** (monthly), NRT for 2023 and 2024	Optimal Interpolation	Hosoda et al., 2008 https://www.jamstec.go.jp/argo_research/dataset/moaagpv/moaa_en.html
NCEI/ NOAA	Argo + others	Not mentioned (°C)	PSS	90°N-90°S (1°x1°), 0-2000m (26 levels), **01/1960 - 12/2023** (monthly), before 2004: only 0-700m available at yearly scale (or 3-months scales) and 0-2000m available at pentadal scale.	Objective Analysis	Levitus et al., 2012 https://www.ncei.noaa.gov/access/global-ocean-heat-content/bin/anomalydata_tm.pl
EN4/ Met Office (4 products available with different XBT/MBT corrections)	Argo + others	Potential (°K)	PSS	89°N-83°S (1°x1°), 5-5350m (42 levels), **01/1900 - 10/2024** (monthly)	Objective Analysis	Good et al., 2013 https://hadleyserver.metoffice.gov.uk/en4/download-en4-2-2.html
IAP	Argo + others	Conservative (°C)	Absolute Salinity (g/kg)	90°N-90°S (1°x1°), 1-6000m (119 levels), **01/1940 - 12/2024** (monthly)	Ensemble Optimal Interpolation combined to models (CMIP5)	Cheng et al., 2017; Cheng and Zhu, 2016 http://www.ocean.iap.ac.cn/pages/dataService/dataService.html
JMA/ MRI	Argo + others	Not mentioned (°C)	PSU	90°N-90°S (1°x1°), 1-2000m (41 levels), **01/1955 - 12/2023** (monthly)	Objective Analysis	Ishii et al., 2017 https://climate.mri-jma.go.jp/pub/ocean/ts/v7.3.1/temp/nc/
CORA5.2/ CMEMS/ OceanScope	Argo + others	Not mentioned (°C)	PSS-78	89°N-77°S (0.12°x0.5°), 1-5500m (187 levels), **01/1960 - 12/2024** (monthly), NRT for 2024	Objective Analysis (ISAS Software)	Cabanes et al., 2013 Delay Mode: https://data.marine.copernicus.eu/product/INSITU_GLO_PHY_TS_OA_MY_013_052/description Near Real Time: https://data.marine.copernicus.eu/product/INSITU_GLO_PHY_TS_OA_NRT_013_002/description
ARMOR3D/ CMEMS/ CLS	Argo + others + satellite (SSH)	Not mentioned (°C)	PSU	89°N-83°S (0.25°x0.25°), 0-5500m (50 levels), **01/1993 - 12/2024** (monthly), NRT for 2023 and 2024	Optimal Interpolation	Guinehut et al., 2012; Mulet et al., 2012 https://data.marine.copernicus.eu/product/MULTIOBS_GLO_PHY_TSUV_3D_MYNRT_015_012/description
RFROM/ PMEL/ NOAA	Argo + others + satellite (SSH and SST)	Conservative (°C)	Not available yet	90°N-90°S (0.25°x0.25°), 2.5-1975m (58 levels), **01/1993 - 12/2023** (7-days)	Random Forest Regression Ocean Maps	(Lyman and Johnson, 2023) https://www.pmel.noaa.gov/rfrom/

310 **Table 2 | In situ Temperature and salinity gridded products at (near-) global scale.**

https://doi.org/10.5194/essd-2026-106
Preprint. Discussion started: 26 February 2026
© Author(s) 2026. CC BY 4.0 License.

3.2.2 Temperature variable definition

A fundamental methodological choice in GOHC estimation concerns the type of temperature variable used. Although in situ temperature is the directly observed quantity and the one typically archived in national databases, most scientific analyses rely instead on potential temperature (θ, under ITS-90; McGlashan, 1990) or conservative temperature (Θ, under TEOS-10; Mcdougall et al., 2010). These derived variables are better suited for estimating heat content, as they correct for pressure effects and/or variations in seawater heat capacity. Despite their importance, many gridded temperature products do not clearly specify which temperature variable they provide. As summarized in Table 2, only a few gridded products (e.g., IPRC, SIO, MOAA GPV, EN4) explicitly report potential temperature, while others (e.g., IAP, RFROM) distribute conservative temperature. Although in situ temperature represents the observed variable, it is not the most appropriate for quantifying heat content, as it can vary with pressure even when the actual heat content remains unchanged (McDougall et al., 2021, 2023a). Potential temperature eliminates these pressure effects but assumes a constant heat capacity, thus providing only an approximation of true heat content. In contrast, conservative temperature is both pressure-independent and thermodynamically consistent with heat content, making it the recommended variable for OHC estimation under TEOS-10.

Despite this theoretical consensus, different approaches continue to exist in the literature. To assess the practical impact of the temperature variable on GOHC, we use the IAP temperature product, which provides conservative temperature (Θ) and absolute salinity (SA). From these variables, we compute both potential temperature (θ) and in situ temperature (T) using the TEOS-10 Gibbs function.

3.2.3 Density and heat capacity assumptions

The treatment of seawater density (ρ) and specific heat capacity (Cp) can also influence GOHC estimates. While many studies assume constant values for these parameters (e.g., Savita et al., 2022), others allow them to vary as a function of salinity, temperature, and pressure (e.g., Meyssignac et al., 2019). To evaluate the sensitivity of GOHC to these assumptions, we tested four configurations: (i) both ρ and Cp are set to be constant; (ii) both vary; (iii) ρ is constant and Cp varies; (iv) ρ varies and Cp is constant. Variable ρ and Cp were computed using the TEOS-10 Gibbs equations (Mcdougall et al., 2010) from absolute salinity (SA), conservative temperature (Θ), in situ temperature (T), and pressure (p). All experiments were performed using the same IAP product for the global 0–2000 m ocean layer. Although constant values for ρ and Cp differ among studies and operational systems (e.g., Boland et al., 2023; Cheng et al., 2022b; Foukal and Lozier, 2018; Huguenin et al., 2022; Savita et al., 2022; Shi et al., 2023; Su et al., 2023) we adopt ρ_0 = 1030 kg m^{-3} and Cp_0 = 3980 J kg^{-1} $°C^{-1}$.

3.2.4 Ocean domain sensitivity

The definition of the ocean domain can also affect the value of GOHC and its associated trend estimates. The spatial coverage of in situ temperature products varies considerably (Table 2). Some datasets encompass the entire global ocean (90°N–90°S), while others are limited to near-global extents (e.g., 60°N–60°S) or exclude specific regions such as shallow seas and polar areas. To enable reproducible assessments and meaningful inter-product comparisons, it is essential to recompute GOHC over a common spatial domain (Jeon, 2021; Savita et al., 2022). In the literature, several strategies have been adopted to define such a common domain. Some studies achieve consistency by applying a single ocean surface mask across all products (e.g., Marti et al., 2022; Minière et al., 2023), while others exclude poorly sampled regions such as the polar oceans or shallow

https://doi.org/10.5194/essd-2026-106
Preprint. Discussion started: 26 February 2026
© Author(s) 2026. CC BY 4.0 License.

continental shelves (von Schuckmann et al., 2020, 2023). Although these approaches enhance the comparability of global OHC estimates by ensuring a more consistent ocean area among products, no study to date has systematically examined the impact of enforcing a consistent ocean volume across all products. In this study, we assess how differing domain definitions affect GOHC estimates by testing six configurations: (i) the native spatial domain of each product; (ii) the global ocean excluding polar latitudes ($|lat| > 60°$); (iii) the global ocean with regions shallower than 300 m masked; (iv) the combination of both the polar latitude and shall-depth masks, corresponding to the domain used in the GCOS international assessment (von Schuckmann et al., 2023); (v) the most restrictive common surface, defined as the intersection of all latitude-longitude grid cells shared across products; and (vi) the most restrictive common volume, defined as the intersection of all latitude–longitude–depth grid cells covered by all products.

3.2.5 Trend method sensitivity

The calculation method used to estimate trends can also affect GOHC estimates. We build on the approaches described in Minière et al. (2023) (see their study for full methodological details), namely Ordinary Least Squares (OLS), Weighted Least Squares (WLS), LOWESS-smoothed, and Quadratic-fit regression methods. In both OLS and WLS regressions, the uncertainty on the estimated trend corresponds to the standard error of the regression slope. In the WLS case, this error is weighted by the observational uncertainties associated with each data point, whereas in the OLS case all points are assigned equal weight. Because residuals of GOHC time series exhibit serial autocorrelation, we apply an AR(1)-based correction factor (Santer et al., 2008) to inflate the standard errors of the regression parameters accordingly. In addition to these individual regressions, we implemented a hybrid "OLS+WLS" approach designed to combine their respective strengths. In this method, the central slope estimate is obtained from an OLS regression, which provides an unbiased linear coefficient and is less sensitive to temporal fluctuations in data uncertainties. The corresponding confidence interval is then computed using WLS, applying the reported GOHC uncertainties as weights. This hybrid approach preserves the robustness of the OLS slope estimate while ensuring proper propagating of observational uncertainties, as achieved by WLS. For the LOWESS and Quadratic approaches, the trend is estimated from a smoothed version of the time series. Associated uncertainties are evaluated via a Monte Carlo procedure (Cheng et al., 2022b): 1,000 surrogate series are generated by adding random noise (with the same variance and autocorrelation structure as the residuals) to the fitted curve, and the spread (standard deviation) of the resulting trends provides the uncertainty estimate. We also include the DELTA method (Palmer et al., 2021), which computes the trend as the difference between the first and last values of the selected period (without prior smoothing, unlike the LOWESS and Quadratic approaches). Uncertainties are propagated by combining, in quadrature, the uncertainties of these two endpoint values. This method is included because it underpins the trend estimates reported in IPCC assessments.

3.3 Results

In this section, we assess the sensitivity of GOHC trends to methodological assumptions, focusing on the period 2005–2020, which is common to all products in our ensemble. Results are shown in Fig. 4. To quantify the impact of each methodological choice, we calculated, for every sensitivity test category (temperature product, temperature variable, density and heat capacity treatment, ocean domain, and trend estimation method), the relative difference between the minimum and maximum trend estimates in W m^{-2}, and expressed as a

https://doi.org/10.5194/essd-2026-106
Preprint. Discussion started: 26 February 2026
© Author(s) 2026. CC BY 4.0 License.

390 percentage of the maximum value. These metrics provide a straightforward measure of how strongly GOHC
391 trends depend on each methodological assumption.

392 The choice of temperature product exerts the strongest influence on GOHC trends, leading to variations of up to
393 47% across datasets. Estimated trends range from 0.38 ± 0.25 W m^{-2} (CORA5.2) to 0.71 ± 0.14 W m^{-2}
394 (EN4.2.2-G10), corresponding to an absolute difference of 0.33 W m^{-2}. Trends also remain sensitive to
395 XBT/MBT bias corrections, even during the Argo era, although the effect is smaller (0.07 W m^{-2} between
396 EN4.2.2-G10 and EN4.2.2-L09). The ensemble mean trend (0.57 ± 0.21 W m^{-2}) encompasses nearly all
397 individual estimates within its uncertainty range, with the exception of CORA5.2, which stands out as an outlier.
398 When excluding CORA5.2, GOHC trends differ by up to 29%, with an absolute difference of 0.21 W m^{-2}
399 between EN4.2.2-G10 and the NOAA estimate (0.50 ± 0.16 W m^{-2}).

400 The definition of the temperature variable has a negligible effect on GOHC trends. Although absolute GOHC
401 values differ depending on whether in situ, potential, or conservative temperature is used (see Fig. S4), the
402 corresponding 2005–2020 trends vary by only 0.003 W m^{-2}, less than 1%.

403 Similarly, the treatment of thermodynamic parameters (ρ, Cp) produces only minor differences: allowing
404 density and heat capacity to vary changes absolute GOHC values (see Fig. S4) but also alters the 0–2000 m
405 trend by just 0.02 W m^{-2}, or about 4%.

406 The definition of ocean domain affects trend estimates by up to 12%. The largest reduction occurs when using
407 the common-volume mask, which yields an absolute difference of 0.07 W m^{-2} relative to the unmasked
408 estimate. Products already limited in spatial coverage (e.g., SIO, CSIO, JAMSTEC) display weaker sensitivity.

409 Sensitivity to the trend estimation method reaches up to 18% (0.11 W m^{-2}), comparable to that found in the
410 ocean domain tests. The choice of method affects both central trend estimates and their associated uncertainties.
411 Among the approaches tested, LOWESS and Quadratic regressions produce the narrowest confidence intervals,
412 while the DELTA method gives the most conservative trend estimate. The hybrid OLS+WLS method represents
413 a balanced compromise: it offers an unbiased slope (unlike WLS, which is affected by GOHC uncertainties) and
414 an uncertainty range broad enough to encompass all other central estimates.

415 In summary, GOHC trends are remarkably robust across methodological configurations. Variations related to
416 the temperature variable, thermodynamic parameters, ocean domain, or trend estimation method remain
417 generally below, or at most on the order of 0.1 W m^{-2}, well within the ensemble-mean uncertainty range of 0.21
418 W m^{-2}. The dominant source of variability in GOHC trends is the choice of temperature product. Although this
419 analysis focuses on the 2005–2020 period, the same conclusion holds for longer timescales (see Fig. S5).

https://doi.org/10.5194/essd-2026-106
Preprint. Discussion started: 26 February 2026
© Author(s) 2026. CC BY 4.0 License.

Open Access Earth System Science Data Discussions

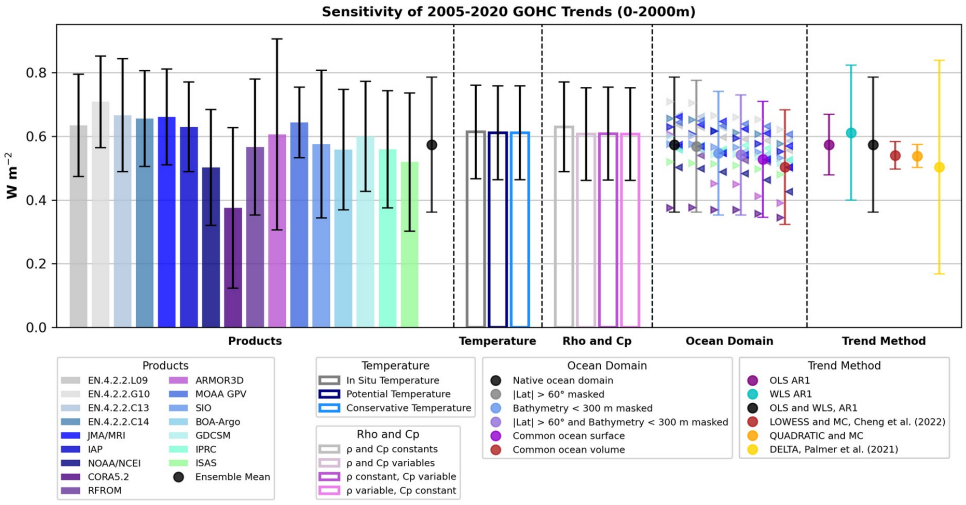

Figure 4 | Method assessment of ocean warming. GOHC trends are estimated over the common period 2005–2020. Five categories of sensitivity tests are conducted: (i) sensitivity to the temperature product used, (ii) sensitivity to the temperature variable definition (in situ, potential, or conservative), (iii) sensitivity to the treatment of seawater density (ρ) and heat capacity (Cp) considered either as constants or as spatially varying fields, (iv) sensitivity to the definition of the ocean domain used for integration, and (v) and sensitivity to the regression method applied for trend estimation. For the product-sensitivity test, trends are computed for each product individually over their native spatial domains, as well as for the ensemble mean (black dot). For the temperature-variable and ρ/Cp sensitivity tests, the IAP product is used. For the ocean-domain test, results are shown for both the ensemble mean (circles) and the individual products (triangles). For the regression-method test, the trend is computed on the ensemble mean only. Error bars represent the 95 % confidence intervals of the trend estimates. Except for the regression-method test, all trends are calculated using the OLS+WLS approach with AR(1) correction.

3.4 Uncertainty assessment of GOHC estimates

Accurately quantifying uncertainties along the chain from raw subsurface temperature measurements to global ocean heat content estimates remains a major challenge. A key limitation lies in the absence of standardized criteria, consistent terminology, and widely accepted best practices for treating uncertainties in Earth and climate observations (Merchant et al., 2017). In particular, the frequent confusion between the terms *error*, *uncertainty*, and *data quality* complicate cross-study comparisons. International initiatives have sought to address this issue. Intercomparison exercises (e.g., Boyer et al., 2016; Savita et al., 2022) have systematically evaluated how mapping techniques, XBT corrections, and baseline climatologies affect OHC estimates at both global and regional scales. Building on these initiatives, the IAPSO MapEval4OceanHeat project now aims to establish best practices for benchmarking mapping methods used to reconstruct OHC and thermosteric sea level (Giglio et al., 2024). Such coordinated frameworks are expected to refine reconstruction methodologies, improve uncertainty quantification, and enhance the robustness of OHC-based indicators of EEI and sea level rise.

https://doi.org/10.5194/essd-2026-106
Preprint. Discussion started: 26 February 2026
© Author(s) 2026. CC BY 4.0 License.

Open Access Earth System Science Data Discussions

447 In this study, we adopt a pragmatic ensemble-based approach to quantify GOHC uncertainty, representing it by
448 the spread (standard deviation) across multiple GOHC estimates. This practice follows the methodology
449 commonly used in IPCC assessments and previous studies (Forster et al., 2021; von Schuckmann et al., 2020,
450 2023). To validate this approach, we compared two types of ensemble spreads (one derived from von
451 Schuckmann et al. (2023) and one calculated in the present study) with product-specific uncertainties provided
452 directly by individual research groups (Fig. 5). These "internal" uncertainties correspond to the uncertainty
453 associated with each GOHC product and require full access to the underlying gridding and product-generation
454 systems. Because such detailed information is rarely available, consistent uncertainty estimation across all
455 products remains infeasible. To date, only a few studies (e.g., Cheng et al., 2017; Levitus et al., 2012; von
456 Schuckmann and Le Traon, 2011) have published product-specific GOHC uncertainty estimates. As an
457 additional line of evidence, we also considered the independent, indirect estimate from Marti et al. (2022),
458 derived from the global sea level budget.
459

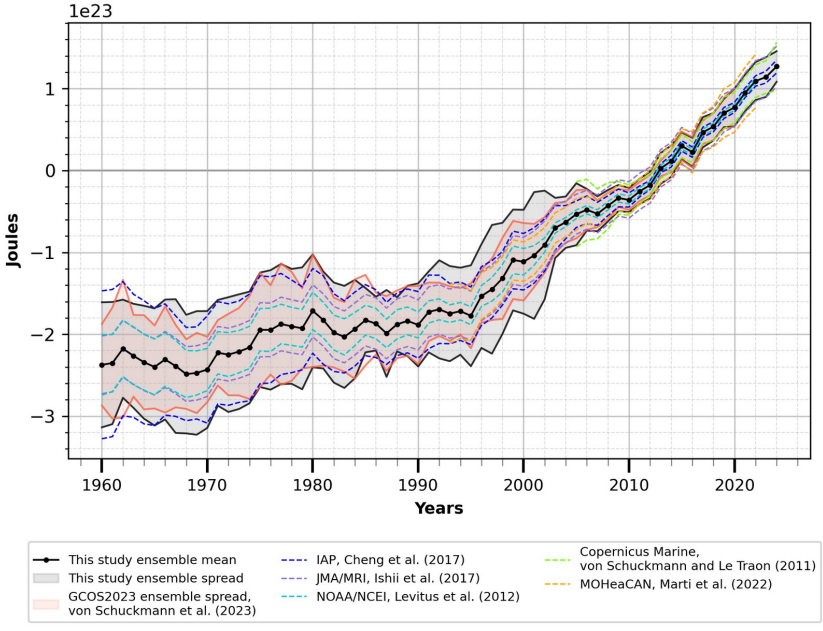

460 **Figure 5 | GOHC uncertainties.** Ensemble-spread uncertainties from this study (black shading and bold lines)
461 and von Schuckmann et al. (2023) (salmon shading and bold lines), are compared with product-specific
462 "internal" uncertainties (dashed lines) reported by Cheng et al. (2017) (dark blue), Levitus et al. (2012) (light
463 blue), Ishii et al. (2017) (purple), von Schuckmann and Le Traon (2011) (green), and Marti et al. (2022)
464 (orange). All uncertainties are given at 95% confidence level.

465 Our comparison shows that the ensemble spread generally encompasses the internal uncertainties reported by
466 individual groups, supporting its use as a practical proxy for GOHC uncertainty (Fig. 5). While this approach is
467 not mathematically rigorous in the strictest sense, it represents the most feasible and transparent compromise
468 under current data constraints. Importantly, the ensemble spread does not underestimate uncertainties compared
469 to the dedicated error envelopes provided by groups that compute them. Future progress will depend on
470 encouraging all data providers to systematically report product-specific GOHC uncertainties, thereby enabling

https://doi.org/10.5194/essd-2026-106
Preprint. Discussion started: 26 February 2026
© Author(s) 2026. CC BY 4.0 License.

more comprehensive intercomparisons and further strengthening ensemble-based approaches. Until such standardization is achieved, the ensemble spread remains a robust and operationally useful method for estimating GOHC uncertainties.

4 Discussion and recommendations

Understanding how methodological assumptions influence GOHC trend estimates is essential for ensuring the robustness and comparability of ocean warming assessments. A central motivation of this study was to clarify the origins of the large spread among published global warming rate estimates (Fig. 1). Our analysis revealed that part of this spread arises from the specific averaging period considered, reflecting the strong multidecadal variability in ocean heating rates (Fig. 2). This variability makes short-term trends highly sensitive to the choice of the averaging window, underscoring the need to interpret present-day EEI values within a broader temporal context. Building on this finding, we further investigated the extent to which methodological choices made during the post-processing part of gridded temperature products could also influence GOHC trend estimates. We systematically tested the sensitivity of GOHC trends to five methodological factors the choice of gridded subsurface temperature product, the definition of temperature variables, the treatment of thermodynamic parameters (ρ, Cp), the selection of the ocean domain, and the statistical approach used to compute trends (Fig. 4).

Our results show that GOHC trends are remarkably robust across methodological configurations. Variations associated with the temperature variable, thermodynamic parameters, ocean domain, or trend estimation method do not exceed approximately 0.1 W m^{-2}, well within the ensemble-mean uncertainty range of 0.21 W m^{-2}. The dominant factor influencing GOHC trend estimates is the choice of the temperature product. These findings demonstrate that, at the global scale, methodological differences exert a much smaller influence than the inter-product spread or ensemble uncertainty, indicating that GOHC trends are both consistent and resilient to post-processing choices. Nevertheless, while these methodological choices have only a moderate influence on global estimates, they can have a substantial impact on regional OHC trends. For this reason, systematic sensitivity testing should be considered a standard component of any regional OHC analysis. Looking ahead, coordinated efforts to standardize methodological practices and transparently document their impacts will be essential to further strengthen the robustness and traceability of this key climate indicator.

These methodological issues are frequently discussed within the GOHC community, particularly concerning the treatment of thermodynamic variables (McDougall et al., 2023b), domain definitions (Jeon, 2021; Savita et al., 2022), and statistical methods (e.g., Cheng et al., 2022b; Palmer et al., 2021). Our results provide quantitative evidence that, at the global scale, methodological diversity introduces only marginal differences compared to product-related uncertainties. Beyond the dominant influence of the temperature product, our sensitivity experiments show that the definition of the temperature variable (in situ, potential, or conservative) and the treatment of thermodynamic parameters (ρ, Cp) have a negligible effect on the global trends, modifying them by less than 0.02 W m^{-2}. By contrast, the choice of ocean domain and the method used to compute trends exert a more noticeable influence. For the ocean domain, we recommend adopting the common mask used by von Schuckmann et al. (2023), which provides a pragmatic balance between ease of implementation and methodological consistency across products.

https://doi.org/10.5194/essd-2026-106
Preprint. Discussion started: 26 February 2026
© Author(s) 2026. CC BY 4.0 License.

Trend estimation deserves particular attention because it underpins key climate metrics derived from GOHC, such as the absolute value of the EEI (von Schuckmann et al., 2016). Several statistical approaches are commonly used within the community, including simple differencing (delta-method), linear regression, LOWESS smoothing, and quadratic fits, each offering different trade-offs between robustness and sensitivity to end effects (Cheng et al., 2022b). Our sensitivity analysis shows that these methods can alter GOHC trend estimates by up to 0.11 W m^{-2} (18%). To mitigate boundary effects while accurately propagating observational uncertainties, we recommend using a hybrid OLS+WLS regression framework, which combines the unbiased slope of OLS with the more realistic uncertainty propagation of WLS.

Uncertainty quantification remains a critical component of GOHC estimation, as it directly determines confidence in derived metrics such as the ocean warming rate or EEI. In this study, we assessed uncertainties by analyzing the spread across multiple gridded subsurface temperature products and comparing the reported internal errors from individual datasets. Our results show that the ensemble spread provides a robust and practical proxy for total uncertainty as it captures both inter-product variability and the “internal” uncertainties reported by individual research groups. Although this approach is not mathematically rigorous in the strictest sense, it represents a feasible and transparent compromise that can be applied consistently across products and does not underestimate uncertainties relative to those reported by groups providing explicit uncertainty envelopes. For these reasons, we recommend adopting the ensemble spread as a standard measure of GOHC uncertainty, as it offers a consistent, reproducible, transparent and broadly applicable framework.

A critical question concerns which GOHC time series should serve as the foundation for a global climate indicator. In practice, two main categories are relevant:

(i) Research-oriented or international reference GOHC indicators, such as the dataset developed in this study or the coordinated GCOS assessment (von Schuckmann et al., 2023), which aim to provide standardized, transparent, and scientifically traceable reference series for long-term climate monitoring;

(ii) Operational or near–real-time indicators, which rely on the most recently available observations, typically up to year N–1 (i.e., the year preceding the current calendar year), and prioritize timeliness for climate monitoring and early warning applications.

Our analysis demonstrates that these different types of GOHC indicators are highly consistent, exhibiting similar trends regardless of the time period considered (Fig. 6). In this study, the research-oriented GOHC time series was derived directly from gridded subsurface temperature products, enabling a detailed evaluation of methodological sensitivities. By contrast, the international GCOS indicator (von Schuckmann et al., 2023) computes the ensemble mean of GOHC time series provided by data producers rather than recalculating them from temperature grids. This approach broadens the ensemble by incorporating estimates for which gridded fields are unavailable, thereby improving representativeness across data providers. Although one might expect differences between the GCOS ensemble mean and the estimate developed here, our results show that both yield nearly identical trends, with discrepancies well within methodological uncertainty. This convergence reinforces confidence in GOHC as a robust and reliable global climate indicator.

https://doi.org/10.5194/essd-2026-106
Preprint. Discussion started: 26 February 2026
© Author(s) 2026. CC BY 4.0 License.

The operational GOHC indicator, based on all gridded temperature products updated to year N–1 (excluding ISAS and IPRC) and including the Copernicus Marine operational indicator (von Schuckmann and Le Traon, 2011), exhibits trends consistent with both the research-oriented and GCOS assessments. This encouraging result demonstrates that a regularly updated, near–real-time GOHC indicator can provide a reliable measure of ongoing ocean warming. It further shows that such an operational framework remains stable even when individual time series are added or removed as data availability evolves. Importantly, adopting an ensemble mean of multiple time series, rather than relying on a single product, provides a more robust estimate of global ocean heat content. It overcomes the limitations of individual datasets and produces a spread that serves as a practical proxy for uncertainty, providing a solid basis for trend assessment. Together, these findings strengthen the case for adopting the operational GOHC indicator in climate monitoring and assessment reports, ensuring both continuity and scientific integrity in tracking EEI.

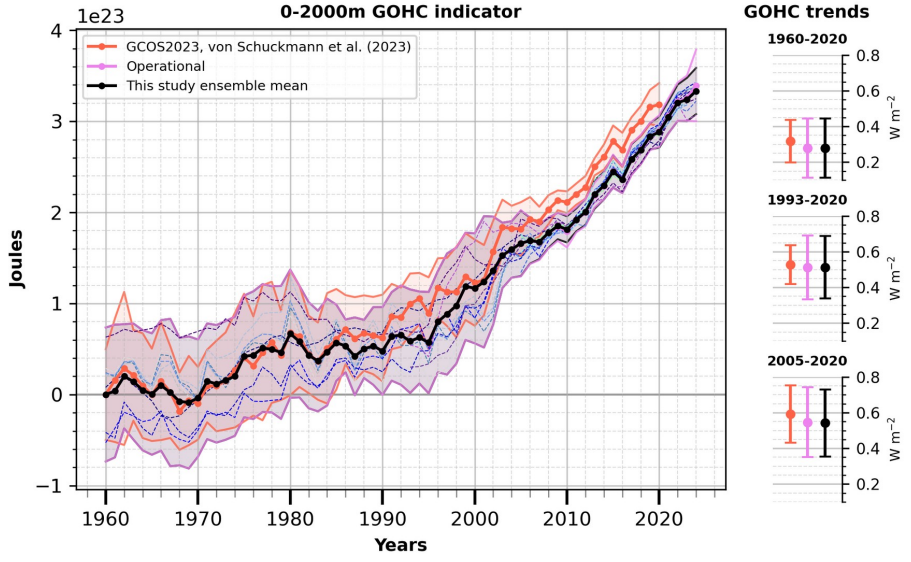

Figure 6 | 0–2000 m GOHC indicator. Comparison of GOHC time series from von Schuckmann et al. (2023) (salmon), the ensemble mean from this study (black), and an operational GOHC estimate including only data available up to year N-1 (pink). All series represent anomalies relative to 1960, calculated over a near-global ocean domain that excludes areas shallower than 300 m and latitudes beyond 60°, with shading indicating twice the ensemble spread. Right panels show trends for 1960–2020, 1993–2020, and 2005–2020, computed using the OLS+WLS method with AR(1) correction and displayed with 95% confidence intervals

Finally, it is essential to emphasize the broader implications of establishing a reliable GOHC indicator. Ocean warming drives fundamental changes in marine systems (Venegas et al., 2023), from heat accumulation in the upper ocean to shifts in stratification (Li et al., 2020; Sallée et al., 2021) and circulation (Mecking and Drijfhout, 2023; Shi et al., 2021), and the increased occurrence of marine heatwaves (Cheng et al., 2022c; Frölicher et al., 2018; Guinaldo et al., 2025; Oliver et al., 2018). Robust and standardized GOHC indicators form a cornerstone for quantifying EEI and for estimating the Earth Heat Inventory (von Schuckmann et al., 2020, 2023). The

https://doi.org/10.5194/essd-2026-106
Preprint. Discussion started: 26 February 2026
© Author(s) 2026. CC BY 4.0 License.

GOHC indicator developed here, along with its associated methodology, can also serve as a benchmark for evaluating and improving ocean reanalyses, including projects such as the Marine Environment Reanalyses Evaluation Project (MER-EP: https://oceandecade.org/actions/marine-environment-reanalyses-evaluation-project/) which aims to assess and enhance the reliability and usability of global and regional ocean reanalyses, and for assessing their fidelity in reproducing historical ocean warming and variability (Balmaseda et al., 2013; Storto et al., 2022). Beyond their diagnostic value, accurate GOHC and EEI estimates derived from observations represent the most direct measure of how the Earth system is actually warming. They provide the physical reference needed to assess CMIP6 simulations, quantify the deep ocean's contribution in global heat uptake, and guide effective adaptation and mitigation strategies.

Code and Data availability

The global ocean heat content time series produced in this manuscript and Python scripts used to process the temperature grids and generate GOHC time series are available at Zenodo: https://doi.org/10.5281/zenodo.18485246 (Minière, 2026). Refer to the README file for instructions on using the codes and datasets, as well as for reproducing the figures presented in the manuscript.

Earth's Energy Imbalance Published Values

Published estimates of EEI used in Figure 1 were manually compiled from the literature and consolidated into a dedicated CSV file archived on Zenodo. This file includes detailed information on the references and the type of estimates. Further details are provided in the README file.

Gridded temperature products

The gridded in situ temperature products used in this study are available from the original providers. Data access links and references are provided in Table 1. These datasets are hosted by the respective institutions and are freely accessible following their conditions.

Bathymetry

To compute the bathymetry mask shallower than 300m, we used the GEBCO 2020 Grid product from the GEBCO Compilation Group (2020) (doi: 10.5285/a29c5465-b138-234d-e053-6c86abc040b9).

GOHC timeseries

The global ocean heat content time series produced in this manuscript were derived from the gridded temperature products listed in Table 1 using the methods described in Section 3 and Section 4.

The GOHC indicator from von Schuckmann et al. (2023) used in Fig. 5 and 6 was downloaded at this link : https://www.wdc-climate.de/ui/entry?acronym=GCOS_EHI_EXP_v2.

In Fig. 5, we use the GOHC uncertainties associated to GOHC indicator distributed by NOAA/NCEI (Levitus et al., 2012, https://www.ncei.noaa.gov/access/global-ocean-heat-content/monthly_analysis.html), JMA/MRI (Ishii et al., 2017, https://www.data.jma.go.jp/kaiyou/english/ohc/ohc_data_en.html), IAP (Cheng et al., 2017, http://www.ocean.iap.ac.cn/pages/dataService/dataService.html), Copernicus Marine (von Schuckmann et al., 2011, https://marine.copernicus.eu/ocean-climate-portal/ocean-heat-content) and AVISO/LEGOS (MOHeaCAN

https://doi.org/10.5194/essd-2026-106
Preprint. Discussion started: 26 February 2026
© Author(s) 2026. CC BY 4.0 License.

product, Marti et al., 2022, https://www.aviso.altimetry.fr/en/data/products/ocean-indicators-products/ocean-heat-content-and-earth-energy-imbalance.html).

Author contributions

AM designed the study, performed the data analysis, developed the codes, generated the figures, and drafted the manuscript, with input from all co-authors. All authors contributed to the interpretation of the results and to revising the manuscript.

Competing interests

The author declares no competing interests.

Disclaimer

Copernicus Publications remains neutral with regard to jurisdictional claims made in the text, published maps, institutional affiliations, or any other geographical representation in this paper. While Copernicus Publications makes every effort to include appropriate place names, the final responsibility lies with the authors. Views expressed in the text are those of the authors and do not necessarily reflect the views of the publisher.

Acknowledgements

The author gratefully acknowledges Flora Gues and Zhetao Tan for their valuable discussions, insightful comments, and helpful advice throughout the development of this study.

Financial support

ObsSea4Clim “Ocean observations and indicators for climate and assessments” is funded by the European Union, Horizon Europe Funding Programme for Research and Innovation under grant agreement number: 101136548. ObsSea4Clim contribution nr. 44.

References

Abraham, J. P., Baringer, M., Bindoff, N. L., Boyer, T., Cheng, L. J., Church, J. A., Conroy, J. L., Domingues, C. M., Fasullo, J. T., Gilson, J., Goni, G., Good, S. A., Gorman, J. M., Gouretski, V., Ishii, M., Johnson, G. C., Kizu, S., Lyman, J. M., Macdonald, A. M., Minkowycz, W. J., Moffitt, S. E., Palmer, M. D., Piola, A. R., Reseghetti, F., Schuckmann, K., Trenberth, K. E., Velicogna, I., and Willis, J. K.: A review of global ocean temperature observations: Implications for ocean heat content estimates and climate change, Rev. Geophys., 51, 450–483, https://doi.org/10.1002/rog.20022, 2013.

Baggenstos, D., Häberli, M., Schmitt, J., Shackleton, S. A., Birner, B., Severinghaus, J. P., Kellerhals, T., and Fischer, H.: Earth’s radiative imbalance from the Last Glacial Maximum to the present, Proc. Natl. Acad. Sci., 116, 14881–14886, https://doi.org/10.1073/pnas.1905447116, 2019.

Bagnell, A. and DeVries, T.: 20th century cooling of the deep ocean contributed to delayed acceleration of Earth’s energy imbalance, Nat. Commun., 12, 4604–4604, https://doi.org/10.1038/s41467-021-24472-3, 2021.

Balmaseda, M. A., Trenberth, K. E., and Källén, E.: Distinctive climate signals in reanalysis of global ocean heat content, Geophys. Res. Lett., 40, 1754–1759, https://doi.org/10.1002/grl.50382, 2013.

https://doi.org/10.5194/essd-2026-106
Preprint. Discussion started: 26 February 2026
© Author(s) 2026. CC BY 4.0 License.

641 Betts, R. A., Belcher, S. E., Hermanson, L., Klein Tank, A., Lowe, J. A., Jones, C. D., Morice, C. P., Rayner, N.
642 A., Scaife, A. A., and Stott, P. A.: Approaching 1.5 °C: how will we know we've reached this crucial warming
643 mark?, Nature, 624, 33–35, https://doi.org/10.1038/d41586-023-03775-z, 2023.

644 Boland, E. J. D., Dittus, A. J., Jones, D. C., Josey, S. A., and Sinha, B.: Ocean Heat Content Responses to
645 Changing Anthropogenic Aerosol Forcing Strength: Regional and Multi-Decadal Variability, J. Geophys. Res.
646 Oceans, 128, e2022JC018725, https://doi.org/10.1029/2022JC018725, 2023.

647 Boyer, T., Domingues, C. M., Good, S. A., Johnson, G. C., Lyman, J. M., Ishii, M., Gouretski, V., Willis, J. K.,
648 Antonov, J., Wijffels, S., Church, J. A., Cowley, R., and Bindoff, N. L.: Sensitivity of Global Upper-Ocean Heat
649 Content Estimates to Mapping Methods, XBT Bias Corrections, and Baseline Climatologies, J. Clim., 29, 4817–
650 4842, https://doi.org/10.1175/JCLI-D-15-0801.1, 2016.

651 Cabanes, C., Grouazel, A., von Schuckmann, K., Hamon, M., Turpin, V., Coatanoan, C., Paris, F., Guinehut, S.,
652 Boone, C., Ferry, N., de Boyer Montégut, C., Carval, T., Reverdin, G., Pouliquen, S., and Le Traon, P.-Y.: The
653 CORA dataset: validation and diagnostics of in-situ ocean temperature and salinity measurements, Ocean Sci.,
654 9, 1–18, https://doi.org/10.5194/os-9-1-2013, 2013.

655 Cheng, L. and Zhu, J.: Influences of the Choice of Climatology on Ocean Heat Content Estimation, J.
656 Atmospheric Ocean. Technol., 32, 388–394, https://doi.org/10.1175/JTECH-D-14-00169.1, 2015.

657 Cheng, L. and Zhu, J.: Benefits of CMIP5 Multimodel Ensemble in Reconstructing Historical Ocean Subsurface
658 Temperature Variations, J. Clim., 29, 5393–5416, https://doi.org/10.1175/JCLI-D-15-0730.1, 2016.

659 Cheng, L., Zhu, J., Cowley, R., Boyer, T., and Wijffels, S.: Time, Probe Type, and Temperature Variable Bias
660 Corrections to Historical Expendable Bathythermograph Observations, J. Atmospheric Ocean. Technol., 31,
661 1793–1825, https://doi.org/10.1175/JTECH-D-13-00197.1, 2014.

662 Cheng, L., Jiang, Z., and Abraham, J.: Global Upper Ocean Heat Content Estimation: Recent Progress and the
663 Remaining Challenges, Atmospheric Ocean. Sci. Lett., 8, 333–338, https://doi.org/10.3878/AOSL20150031,
664 2015.

665 Cheng, L., Trenberth, K. E., Fasullo, J., Boyer, T., Abraham, J., and Zhu, J.: Improved estimates of ocean heat
666 content from 1960 to 2015, Sci. Adv., 3, e1601545, https://doi.org/10.1126/sciadv.1601545, 2017.

667 Cheng, L., Abraham, J., Trenberth, K. E., Fasullo, J., Boyer, T., Mann, M. E., Zhu, J., Wang, F., Locarnini, R.,
668 Li, Y., Zhang, B., Tan, Z., Yu, F., Wan, L., Chen, X., Song, X., Liu, Y., Reseghetti, F., Simoncelli, S.,
669 Gouretski, V., Chen, G., Mishonov, A., and Reagan, J.: Another Record: Ocean Warming Continues through
670 2021 despite La Niña Conditions, Adv. Atmospheric Sci., 39, 373–385, https://doi.org/10.1007/s00376-022-
671 1461-3, 2022a.

672 Cheng, L., Foster, G., Hausfather, Z., Trenberth, K. E., and Abraham, J.: Improved Quantification of the Rate of
673 Ocean Warming, J. Clim., 35, 4827–4840, https://doi.org/10.1175/JCLI-D-21-0895.1, 2022b.

674 Cheng, L., von Schuckmann, K., Abraham, J. P., Trenberth, K. E., Mann, M. E., Zanna, L., England, M. H.,
675 Zika, J. D., Fasullo, J. T., Yu, Y., Pan, Y., Zhu, J., Newsom, E. R., Bronselaer, B., and Lin, X.: Past and future
676 ocean warming, Nat. Rev. Earth Environ., 3, 776–794, https://doi.org/10.1038/s43017-022-00345-1, 2022c.

677 Cheng, L., Abraham, J., Trenberth, K. E., Reagan, J., Zhang, H.-M., Storto, A., Von Schuckmann, K., Pan, Y.,
678 Zhu, Y., Mann, M. E., Zhu, J., Wang, F., Yu, F., Locarnini, R., Fasullo, J., Huang, B., Graham, G., Yin, X.,
679 Gouretski, V., Zheng, F., Li, Y., Zhang, B., Wan, L., Chen, X., Wang, D., Feng, L., Song, X., Liu, Y.,
680 Reseghetti, F., Simoncelli, S., Chen, G., Zhang, R., Mishonov, A., Tan, Z., Wei, W., Yuan, H., Li, G., Ren, Q.,
681 Cao, L., Lu, Y., Du, J., Lyu, K., Sulaiman, A., Mayer, M., Wang, H., Ma, Z., Bao, S., Yan, H., Liu, Z., Yang,
682 C., Liu, X., Hausfather, Z., Szekely, T., and Gues, F.: Record High Temperatures in the Ocean in 2024, Adv.
683 Atmospheric Sci., https://doi.org/10.1007/s00376-025-4541-3, 2025.

684 Cuesta-Valero, F. J., García-García, A., Beltrami, H., and Finnis, J.: First assessment of the earth heat inventory
685 within CMIP5 historical simulations, Earth Syst. Dyn., 12, 581–600, https://doi.org/10.5194/esd-12-581-2021,
686 2021.

687 Forster, P., Storelvmo, T., Armour, K., Collins, W., Dufresne, J.-L., Frame, D., Lunt, D. J., Mauritsen, T.,
688 Palmer, M. D., Watanabe, M., Wild, M., and Zhang, H.: The Earth's Energy Budget, Climate Feedbacks, and

https://doi.org/10.5194/essd-2026-106
Preprint. Discussion started: 26 February 2026
© Author(s) 2026. CC BY 4.0 License.

Climate Sensitivity, edited by: Masson-Delmotte, V., Zhai, P., Pirani, A., Connors, S. L., Péan, C., Berger, S., Caud, N., Chen, Y., Goldfarb, L., Gomis, M. I., Huang, M., Leitzell, K., Lonnoy, E., Matthews, J. B. R., Maycock, T. K., Waterfield, T., Yelekçi, O., Yu, R., and Zhou, B., Clim. Change 2021 Phys. Sci. Basis Contrib. Work. Group Sixth Assess. Rep. Intergov. Panel Clim. Change, 923–1054, https://doi.org/10.1017/9781009157896.009, 2021.

Forster, P. M., Smith, C., Walsh, T., Lamb, W., Lamboll, R., Hall, B., Hauser, M., Ribes, A., Rosen, D., Gillett, N., Palmer, M. D., Rogelj, J., von Schuckmann, K., Trewin, B., Allen, M., Andrew, R., Betts, R., Boyer, T., Buontempo, C., Burgess, S., Cagnazzo, C., Cheng, L., Friedlingstein, P., Gettelman, A., Gütschow, J., Ishii, M., Jenkins, S., Lan, X., Morice, C., Mühle, J., Kadow, C., Kennedy, J., Killick, R., Krummel, P. B., Minx, J. C., Myhre, G., Naik, V., Peters, G. P., Pirani, A., Pongratz, J., Schleussner, C.-F., Seneviratne, S. I., Szopa, S., Thorne, P., Kovilakam, M. V. M., Majamäki, E., Jalkanen, J.-P., van Marle, M., Hoesly, R. M., Rohde, R., Schumacher, D., van der Werf, G., Vose, R., Zickfeld, K., Zhang, X., Masson-Delmotte, V., and Zhai, P.: Indicators of Global Climate Change 2023: annual update of key indicators of the state of the climate system and human influence, Earth Syst. Sci. Data Discuss., 1–57, https://doi.org/10.5194/essd-2024-149, 2024.

Foukal, N. P. and Lozier, M. S.: Examining the Origins of Ocean Heat Content Variability in the Eastern North Atlantic Subpolar Gyre, Geophys. Res. Lett., 45, 11,275-11,283, https://doi.org/10.1029/2018GL079122, 2018.

Frölicher, T. L., Fischer, E. M., and Gruber, N.: Marine heatwaves under global warming, Nature, 560, 360–364, https://doi.org/10.1038/s41586-018-0383-9, 2018.

Gaillard, F., Reynaud, T., Thierry, V., Kolodziejczyk, N., and Schuckmann, K. von: In Situ–Based Reanalysis of the Global Ocean Temperature and Salinity with ISAS: Variability of the Heat Content and Steric Height, J. Clim., 29, 1305–1323, https://doi.org/10.1175/JCLI-D-15-0028.1, 2016.

Giglio, D., Domingues, C. M., Monselesan, D., Palmer, M. D., Asselot, R., Boyer, T., Forget, G., Goes, M. P., Hakuba, M. Z., Hermanson, L., Johnson, G. C., Killick, R. E., Kolodziejczyk, N., Kuusela, M., Llovel, W., Lyman, J. M., Meyssignac, B., Mills, W., Sebastien, F., Smith, D. M., Sukanto, T., and Troupin, C.: MapEval4OceanHeat: an objective assessment of mapping methods used to estimate ocean heat content change, American Geophysical Union, Ocean Sciences Meeting, ADS Bibcode: 2024AGUOSCC44B1343G, CC44B-1343, 2024.

Good, S. A., Martin, M. J., and Rayner, N. A.: EN4: Quality controlled ocean temperature and salinity profiles and monthly objective analyses with uncertainty estimates, J. Geophys. Res. Oceans, 118, 6704–6716, https://doi.org/10.1002/2013JC009067, 2013.

Gouretski, V. and Cheng, L.: Correction for Systematic Errors in the Global Dataset of Temperature Profiles from Mechanical Bathythermographs, J. Atmospheric Ocean. Technol., 37, 841–855, https://doi.org/10.1175/JTECH-D-19-0205.1, 2020.

Guinaldo, T., Cassou, C., Sallée, J.-B., and Liné, A.: Internal variability effect doped by climate change drove the 2023 marine heat extreme in the North Atlantic, Commun. Earth Environ., 6, 1–11, https://doi.org/10.1038/s43247-025-02197-1, 2025.

Guinehut, S., Dhomps, A.-L., Larnicol, G., and Le Traon, P.-Y.: High resolution 3-D temperature and salinity fields derived from in situ and satellite observations, Ocean Sci., 8, 845–857, https://doi.org/10.5194/os-8-845-2012, 2012.

Gulev, S. K., Thorne, P. W., Ahn, J., Dentener, F. J., Domingues, C. M., Gerland, S., Gong, D., Kaufman, D. S., Nnamchi, H. C., Quaas, J., Rivera, J. A., Sathyendranath, S., Smith, S. L., Trewin, B., von Shuckmann, K., and Vose, R. S.: Changing state of the climate system, in: Climate Change 2021: The Physical Science Basis. Contribution of Working Group I to the Sixth Assessment Report of the Intergovernmental Panel on Climate Change, edited by: Masson-Delmotte, V., Zhai, P., Pirani, A., Connors, S. L., Péan, C., Berger, S., Caud, N., Chen, Y., Goldfarb, L., Gomis, M. I., Huang, M., Leitzell, K., Lonnoy, E., Matthews, J. B. R., Maycock, T. K., Waterfield, T., Yelekçi, Ö., Yu, R., and Zhou, B., Cambridge University Press, Cambridge, United Kingdom and New York, NY, USA, 287–422, https://doi.org/10.1017/9781009157896.001, 2021.

Hakuba, M. Z., Frederikse, T., and Landerer, F. W.: Earth's Energy Imbalance From the Ocean Perspective (2005–2019), Geophys. Res. Lett., 48, e2021GL093624, https://doi.org/10.1029/2021GL093624, 2021.

Hakuba, M. Z., Fourest, S., Boyer, T., Meyssignac, B., Carton, J. A., Forget, G., Cheng, L., Giglio, D., Johnson, G. C., Kato, S., Killick, R. E., Kolodziejczyk, N., Kuusela, M., Landerer, F., Llovel, W., Locarnini, R., Loeb,

https://doi.org/10.5194/essd-2026-106
Preprint. Discussion started: 26 February 2026
© Author(s) 2026. CC BY 4.0 License.

740 N., Lyman, J. M., Mishonov, A., Pilewskie, P., Reagan, J., Storto, A., Sukianto, T., and von Schuckmann, K.:
741 Trends and Variability in Earth's Energy Imbalance and Ocean Heat Uptake Since 2005, Surv. Geophys.,
742 https://doi.org/10.1007/s10712-024-09849-5, 2024.

743 Hansen, J., Nazarenko, L., Ruedy, R., Sato, M., Willis, J., Del Genio, A., Koch, D., Lacis, A., Lo, K., Menon,
744 S., Novakov, T., Perlwitz, J., Russell, G., Schmidt, G. A., and Tausnev, N.: Earth's Energy Imbalance:
745 Confirmation and Implications, Science, 308, 1431–1435, https://doi.org/10.1126/science.1110252, 2005.

746 Hosoda, S., Ohira, T., and Nakamura, T.: A monthly mean dataset of global oceanic temperature and salinity
747 derived from Argo float observations, JAMSTEC Rep. Res. Dev., 8, 47–59,
748 https://doi.org/10.5918/jamstecr.8.47, 2008.

749 Huguenin, M. F., Holmes, R. M., and England, M. H.: Drivers and distribution of global ocean heat uptake over
750 the last half century, Nat. Commun., 13, 4921, https://doi.org/10.1038/s41467-022-32540-5, 2022.

751 Intergovernmental Panel on Climate Change (IPCC) (Ed.): Framing and Context, in: Global Warming of 1.5°C:
752 IPCC Special Report on Impacts of Global Warming of 1.5°C above Pre-industrial Levels in Context of
753 Strengthening Response to Climate Change, Sustainable Development, and Efforts to Eradicate Poverty,
754 Cambridge University Press, Cambridge, 49–92, https://doi.org/10.1017/9781009157940.003, 2022.

755 IPCC: Climate Change 2021: The Physical Science Basis. Contribution of Working Group I to the Sixth
756 Assessment Report of the Intergovernmental Panel on Climate Change, , In Press,
757 https://doi.org/10.1017/9781009157896, 2021.

758 Ishii, M., Fukuda, Y., Hirahara, S., Yasui, S., Suzuki, T., and Sato, K.: Accuracy of Global Upper Ocean Heat
759 Content Estimation Expected from Present Observational Data Sets, Sola, 13, 163–167,
760 https://doi.org/10.2151/sola.2017-030, 2017.

761 Jeon, T.: Impact of Ocean Domain Definition on Sea Level Budget, Remote Sens., 13, 3206,
762 https://doi.org/10.3390/rs13163206, 2021.

763 Kolodziejczyk, N., Prigent-Mazella, A., and Gaillard, F.: ISAS temperature and salinity gridded fields,
764 https://doi.org/10.17882/52367, 2021.

765 Lellouche, J.-M., Eric, G., Romain, B.-B., Gilles, G., Angélique, M., Marie, D., Clément, B., Mathieu, H.,
766 Olivier, L. G., Charly, R., Tony, C., Charles-Emmanuel, T., Florent, G., Giovanni, R., Mounir, B., Yann, D.,
767 and Pierre-Yves, L. T.: The Copernicus Global 1/12° Oceanic and Sea Ice GLORYS12 Reanalysis, Front. Earth
768 Sci., 9, https://doi.org/10.3389/feart.2021.698876, 2021.

769 Levitus, S., Antonov, J. I., Boyer, T. P., Baranova, O. K., Garcia, H. E., Locarnini, R. A., Mishonov, A. V.,
770 Reagan, J. R., Seidov, D., Yarosh, E. S., and Zweng, M. M.: World ocean heat content and thermosteric sea
771 level change (0–2000 m), 1955–2010, Geophys. Res. Lett., 39, https://doi.org/10.1029/2012GL051106, 2012.

772 Li, G., Cheng, L., Zhu, J., Trenberth, K. E., Mann, M. E., and Abraham, J. P.: Increasing ocean stratification
773 over the past half-century, Nat. Clim. Change, 10, 1116–1123, https://doi.org/10.1038/s41558-020-00918-2,
774 2020.

775 Li, H., Xu, F., Zhou, W., Wang, D., Wright, J. S., Liu, Z., and Lin, Y.: Development of a global gridded Argo
776 data set with Barnes successive corrections, J. Geophys. Res. Oceans, 122, 866–889,
777 https://doi.org/10.1002/2016JC012285, 2017.

778 Li, Y., Church, J. A., McDougall, T. J., and Barker, P. M.: Sensitivity of Observationally Based Estimates of
779 Ocean Heat Content and Thermal Expansion to Vertical Interpolation Schemes, Geophys. Res. Lett., 49,
780 e2022GL101079, https://doi.org/10.1029/2022GL101079, 2022.

781 Liang, X., Liu, C., Ponte, R. M., and Chambers, D. P.: A Comparison of the Variability and Changes in Global
782 Ocean Heat Content from Multiple Objective Analysis Products during the Argo Period, J. Clim., 34, 7875–
783 7895, https://doi.org/10.1175/JCLI-D-20-0794.1, 2021.

784 Loeb, N. G., Johnson, G. C., Thorsen, T. J., Lyman, J. M., Rose, F. G., and Kato, S.: Satellite and Ocean Data
785 Reveal Marked Increase in Earth's Heating Rate, Geophys. Res. Lett., 48, e2021GL093047,
786 https://doi.org/10.1029/2021GL093047, 2021.

https://doi.org/10.5194/essd-2026-106
Preprint. Discussion started: 26 February 2026
© Author(s) 2026. CC BY 4.0 License.

787 Lyman, J. M. and Johnson, G. C.: Estimating Annual Global Upper-Ocean Heat Content Anomalies despite
788 Irregular In Situ Ocean Sampling, J. Clim., 21, 5629–5641, https://doi.org/10.1175/2008JCLI2259.1, 2008.

789 Lyman, J. M. and Johnson, G. C.: Estimating Global Ocean Heat Content Changes in the Upper 1800 m since
790 1950 and the Influence of Climatology Choice, J. Clim., 27, 1945–1957, https://doi.org/10.1175/JCLI-D-12-
791 00752.1, 2014.

792 Lyman, J. M. and Johnson, G. C.: Global High-Resolution Random Forest Regression Maps of Ocean Heat
793 Content Anomalies Using In Situ and Satellite Data, J. Atmospheric Ocean. Technol., 40, 575–586,
794 https://doi.org/10.1175/JTECH-D-22-0058.1, 2023.

795 Lyman, J. M., Good, S. A., Gouretski, V. V., Ishii, M., Johnson, G. C., Palmer, M. D., Smith, D. M., and Willis,
796 J. K.: Robust warming of the global upper ocean, Nature, 465, 334–337, https://doi.org/10.1038/nature09043,
797 2010.

798 Ma, X., Liu, W., Allen, R. J., Huang, G., and Li, X.: Dependence of regional ocean heat uptake on
799 anthropogenic warming scenarios, Sci. Adv., 6, eabc0303, https://doi.org/10.1126/sciadv.abc0303, 2020.

800 Marti, F., Blazquez, A., Meyssignac, B., Ablain, M., Barnoud, A., Fraudeau, R., Jugier, R., Chenal, J., Larnicol,
801 G., Pfeffer, J., Restano, M., and Benveniste, J.: Monitoring the ocean heat content change and the Earth energy
802 imbalance from space altimetry and space gravimetry, Earth Syst. Sci. Data, 14, 229–249,
803 https://doi.org/10.5194/essd-14-229-2022, 2022.

804 Marti, F., Meyssignac, B., Rousseau, V., Ablain, M., Fraudeau, R., Blazquez, A., and Fourest, S.: Monitoring
805 global ocean heat content from space geodetic observations to estimate the Earth energy imbalance, State Planet,
806 4-osr8, 1–10, https://doi.org/10.5194/sp-4-osr8-3-2024, 2024.

807 Mcdougall, T., Feistel, R., Millero, F., Jackett, D. R., Wright, D., King, B., Marion, G., Chen, C.-T. A., and
808 Spitzer, P.: The International Thermodynamic Equation of Seawater 2010 (TEOS-10): Calculation and Use of
809 Thermodynamic Properties, 2010.

810 McDougall, T. J., Barker, P. M., Holmes, R. M., Pawlowicz, R., Griffies, S. M., and Durack, P. J.: The
811 interpretation of temperature and salinity variables in numerical ocean model output and the calculation of heat
812 fluxes and heat content, Geosci. Model Dev., 14, 6445–6466, https://doi.org/10.5194/gmd-14-6445-2021, 2021.

813 McDougall, T. J., Barker, P. M., Feistel, R., and Roquet, F.: A thermodynamic potential of seawater in terms of
814 Absolute Salinity, Conservative Temperature, and in situ pressure, Ocean Sci., 19, 1719–1741,
815 https://doi.org/10.5194/os-19-1719-2023, 2023a.

816 McDougall, T. J., Barker, P., Feistel, R., and Roquet, F.: A Thermodynamic Potential of Seawater in terms of
817 Conservative Temperature, EGUsphere, 1–30, https://doi.org/10.5194/egusphere-2023-1568, 2023b.

818 McGlashan, M. L.: The international temperature scale of 1990 (ITS-90), J. Chem. Thermodyn., 22, 653–663,
819 https://doi.org/10.1016/0021-9614(90)90018-L, 1990.

820 Mecking, J. V. and Drijfhout, S. S.: The decrease in ocean heat transport in response to global warming, Nat.
821 Clim. Change, 1–8, https://doi.org/10.1038/s41558-023-01829-8, 2023.

822 Merchant, C. J., Paul, F., Popp, T., Ablain, M., Bontemps, S., Defourny, P., Hollmann, R., Lavergne, T., Laeng,
823 A., de Leeuw, G., Mittaz, J., Poulsen, C., Povey, A. C., Reuter, M., Sathyendranath, S., Sandven, S., Sofieva, V.
824 F., and Wagner, W.: Uncertainty information in climate data records from Earth observation, Earth Syst. Sci.
825 Data, 9, 511–527, https://doi.org/10.5194/essd-9-511-2017, 2017.

826 Merchant, C. J., Allan, R. P., and Embury, O.: Quantifying the acceleration of multidecadal global sea surface
827 warming driven by Earth's energy imbalance, Environ. Res. Lett., 20, 024037, https://doi.org/10.1088/1748-
828 9326/adaa8a, 2025.

829 Meyssignac, B., Boyer, T., Zhao, Z., Hakuba, M. Z., Landerer, F. W., Stammer, D., Köhl, A., Kato, S.,
830 L'Ecuyer, T., Ablain, M., Abraham, J. P., Blazquez, A., Cazenave, A., Church, J. A., Cowley, R., Cheng, L.,
831 Domingues, C. M., Giglio, D., Gouretski, V., Ishii, M., Johnson, G. C., Killick, R. E., Legler, D., Llovel, W.,
832 Lyman, J., Palmer, M. D., Piotrowicz, S., Purkey, S. G., Roemmich, D., Roca, R., Savita, A., Schuckmann, K.

https://doi.org/10.5194/essd-2026-106
Preprint. Discussion started: 26 February 2026
© Author(s) 2026. CC BY 4.0 License.

von, Speich, S., Stephens, G., Wang, G., Wijffels, S. E., and Zilberman, N.: Measuring Global Ocean Heat Content to Estimate the Earth Energy Imbalance, Front. Mar. Sci., 6, 2019.

Minière, A.: Dataset and scripts supporting Consolidating Global Estimates of Ocean Heat Content: Toward a Consistent Earth Heat Inventory, https://doi.org/10.5281/zenodo.18485246, 2026.

Minière, A., von Schuckmann, K., Sallée, J.-B., and Vogt, L.: Robust acceleration of Earth system heating observed over the past six decades, Sci. Rep., 13, 22975, https://doi.org/10.1038/s41598-023-49353-1, 2023.

Minobe, S., Behrens, E., Findell, K. L., Loeb, N. G., Meyssignac, B., and Sutton, R.: Global and regional drivers for exceptional climate extremes in 2023-2024: beyond the new normal, Npj Clim. Atmospheric Sci., 8, 1–11, https://doi.org/10.1038/s41612-025-00996-z, 2025.

Mulet, S., Rio, M.-H., Mignot, A., Guinehut, S., and Morrow, R.: A new estimate of the global 3D geostrophic ocean circulation based on satellite data and in-situ measurements, Deep Sea Res. Part II Top. Stud. Oceanogr., 77–80, 70–81, https://doi.org/10.1016/j.dsr2.2012.04.012, 2012.

Oliver, E. C. J., Donat, M. G., Burrows, M. T., Moore, P. J., Smale, D. A., Alexander, L. V., Benthuysen, J. A., Feng, M., Sen Gupta, A., Hobday, A. J., Holbrook, N. J., Perkins-Kirkpatrick, S. E., Scannell, H. A., Straub, S. C., and Wernberg, T.: Longer and more frequent marine heatwaves over the past century, Nat. Commun., 9, 1324, https://doi.org/10.1038/s41467-018-03732-9, 2018.

Palmer, M. D., Domingues, C. M., Slangen, A. B. A., and Dias, F. B.: An ensemble approach to quantify global mean sea-level rise over the 20th century from tide gauge reconstructions, Environ. Res. Lett., 16, 044043, https://doi.org/10.1088/1748-9326/abdaec, 2021.

Pan, Y., Minière, A., Schuckmann, K., Li, Z., Li, Y., Cheng, L., and Zhu, J.: Ocean heat content in 2024, Nat. Rev. Earth Environ., 6, 249–251, https://doi.org/10.1038/s43017-025-00655-0, 2025.

Pörtner, H.-O., Roberts, D. C., Masson-Delmotte, V., Zhai, P., Tignor, M., Poloczanska, E., Mintenbeck, K., Alegría, A., Nicolai, M., Okem, A., Petzold, J., Rama, B., and Weyer, N. M. (Eds.): IPCC special report on the ocean and cryosphere in a changing climate, Cambridge University Press, Cambridge, UK and New York, NY, USA, https://doi.org/10.1017/9781009157964, 2019.

Resplandy, L., Keeling, R. F., Eddebbar, Y., Brooks, M., Wang, R., Bopp, L., Long, M. C., Dunne, J. P., Koeve, W., and Oschlies, A.: Quantification of ocean heat uptake from changes in atmospheric O2 and CO2 composition, Sci. Rep., 9, 20244, https://doi.org/10.1038/s41598-019-56490-z, 2019.

Rockström, J., Donges, J. F., Fetzer, I., Martin, M. A., Wang-Erlandsson, L., and Richardson, K.: Planetary Boundaries guide humanity's future on Earth, Nat. Rev. Earth Environ., 5, 773–788, https://doi.org/10.1038/s43017-024-00597-z, 2024.

Roemmich, D. and Gilson, J.: The 2004–2008 mean and annual cycle of temperature, salinity, and steric height in the global ocean from the Argo Program, Prog. Oceanogr., 82, 81–100, https://doi.org/10.1016/j.pocean.2009.03.004, 2009.

Sallée, J.-B., Pellichero, V., Akhoudas, C., Pauthenet, E., Vignes, L., Schmidtko, S., Garabato, A. N., Sutherland, P., and Kuusela, M.: Summertime increases in upper-ocean stratification and mixed-layer depth, Nature, 591, 592–598, https://doi.org/10.1038/s41586-021-03303-x, 2021.

Santer, B. D., Thorne, P. W., Haimberger, L., Taylor, K. E., Wigley, T. M. L., Lanzante, J. R., Solomon, S., Free, M., Gleckler, P. J., Jones, P. D., Karl, T. R., Klein, S. A., Mears, C., Nychka, D., Schmidt, G. A., Sherwood, S. C., and Wentz, F. J.: Consistency of modelled and observed temperature trends in the tropical troposphere, Int. J. Climatol., 28, 1703–1722, https://doi.org/10.1002/joc.1756, 2008.

Savita, A., Domingues, C. M., Boyer, T., Gouretski, V., Ishii, M., Johnson, G. C., Lyman, J. M., Willis, J. K., Marsland, S. J., Hobbs, W., Church, J. A., Monselesan, D. P., Dobrohotoff, P., Cowley, R., and Wijffels, S. E.: Quantifying Spread in Spatiotemporal Changes of Upper-Ocean Heat Content Estimates: An Internationally Coordinated Comparison, J. Clim., 35, 851–875, https://doi.org/10.1175/JCLI-D-20-0603.1, 2022.

von Schuckmann, K. and Le Traon, P.-Y.: How well can we derive Global Ocean Indicators from Argo data?, Ocean Sci., 7, 783–791, https://doi.org/10.5194/os-7-783-2011, 2011.

https://doi.org/10.5194/essd-2026-106
Preprint. Discussion started: 26 February 2026
© Author(s) 2026. CC BY 4.0 License.

von Schuckmann, K., Palmer, M. D., Trenberth, K. E., Cazenave, A., Chambers, D., Champollion, N., Hansen, J., Josey, S. A., Loeb, N., Mathieu, P.-P., Meyssignac, B., and Wild, M.: An imperative to monitor Earth's energy imbalance, Nat. Clim. Change, 6, 138–144, https://doi.org/10.1038/nclimate2876, 2016.

von Schuckmann, K., Cheng, L., Palmer, M. D., Hansen, J., Tassone, C., Aich, V., Adusumilli, S., Beltrami, H., Boyer, T., Cuesta-Valero, F. J., Desbruyères, D., Domingues, C., García-García, A., Gentine, P., Gilson, J., Gorfer, M., Haimberger, L., Ishii, M., Johnson, G. C., Killick, R., King, B. A., Kirchengast, G., Kolodziejczyk, N., Lyman, J., Marzeion, B., Mayer, M., Monier, M., Monselesan, D. P., Purkey, S., Roemmich, D., Schweiger, A., Seneviratne, S. I., Shepherd, A., Slater, D. A., Steiner, A. K., Straneo, F., Timmermans, M.-L., and Wijffels, S. E.: Heat stored in the Earth system: where does the energy go?, Earth Syst. Sci. Data, 12, 2013–2041, https://doi.org/10.5194/essd-12-2013-2020, 2020.

von Schuckmann, K., Minière, A., Gues, F., Cuesta-Valero, F. J., Kirchengast, G., Adusumilli, S., Straneo, F., Ablain, M., Allan, R. P., Barker, P. M., Beltrami, H., Blazquez, A., Boyer, T., Cheng, L., Church, J., Desbruyeres, D., Dolman, H., Domingues, C. M., García-García, A., Giglio, D., Gilson, J. E., Gorfer, M., Haimberger, L., Hakuba, M. Z., Hendricks, S., Hosoda, S., Johnson, G. C., Killick, R., King, B., Kolodziejczyk, N., Korosov, A., Krinner, G., Kuusela, M., Landerer, F. W., Langer, M., Lavergne, T., Lawrence, I., Li, Y., Lyman, J., Marti, F., Marzeion, B., Mayer, M., MacDougall, A. H., McDougall, T., Monselesan, D. P., Nitzbon, J., Otosaka, I., Peng, J., Purkey, S., Roemmich, D., Sato, K., Sato, K., Savita, A., Schweiger, A., Shepherd, A., Seneviratne, S. I., Simons, L., Slater, D. A., Slater, T., Steiner, A. K., Suga, T., Szekely, T., Thiery, W., Timmermans, M.-L., Vanderkelen, I., Wjiffels, S. E., Wu, T., and Zemp, M.: Heat stored in the Earth system 1960–2020: where does the energy go?, Earth Syst. Sci. Data, 15, 1675–1709, https://doi.org/10.5194/essd-15-1675-2023, 2023.

Shackleton, S., Seltzer, A., Baggenstos, D., and Lisiecki, L. E.: Benthic δ18O records Earth's energy imbalance, Nat. Geosci., 16, 797–802, https://doi.org/10.1038/s41561-023-01250-y, 2023.

Shackleton, S., Hishamunda, V., Yan, Y., Carter, A., Morgan, J., Severinghaus, J., Aarons, S., Peterson, J. M., Epifanio, J., Buizert, C., Brook, E., Kurbatov, A., Bender, M., and Higgins, J.: Global ocean heat content over the past 3 million years, https://doi.org/10.21203/rs.3.rs-5610580/v1, 6 January 2025.

Shi, J.-R., Talley, L. D., Xie, S.-P., Peng, Q., and Liu, W.: Ocean warming and accelerating Southern Ocean zonal flow, Nat. Clim. Change, 11, 1090–1097, https://doi.org/10.1038/s41558-021-01212-5, 2021.

Shi, J.-R., Wijffels, S. E., Kwon, Y.-O., and Xie, S.-P.: Interhemispheric Contrasts of Ocean Heat Content Change Reveals Distinct Fingerprints of Anthropogenic Climate Forcings, Geophys. Res. Lett., 50, e2023GL102741, https://doi.org/10.1029/2023GL102741, 2023.

Smith, D. M., Allan, R. P., Coward, A. C., Eade, R., Hyder, P., Liu, C., Loeb, N. G., Palmer, M. D., Roberts, C. D., and Scaife, A. A.: Earth's energy imbalance since 1960 in observations and CMIP5 models, Geophys. Res. Lett., 42, 1205–1213, https://doi.org/10.1002/2014GL062669, 2015.

Stammer, D., Sena-Martins, M., Köhler, J., and Köhl, A.: How well do we know ocean salinity and its changes?, Prog. Oceanogr., 190, 102478, https://doi.org/10.1016/j.pocean.2020.102478, 2021.

Storto, A. and Yang, C.: Acceleration of the ocean warming from 1961 to 2022 unveiled by large-ensemble reanalyses, Nat. Commun., 15, 545, https://doi.org/10.1038/s41467-024-44749-7, 2024.

Storto, A., Cheng, L., and Yang, C.: Revisiting the 2003–18 Deep Ocean Warming through Multiplatform Analysis of the Global Energy Budget, J. Clim., 35, 4701–4717, https://doi.org/10.1175/JCLI-D-21-0726.1, 2022.

Su, H., Qin, T., Wang, A., and Lu, W.: Reconstructing Ocean Heat Content for Revisiting Global Ocean Warming from Remote Sensing Perspectives, Remote Sens., 13, 3799, https://doi.org/10.3390/rs13193799, 2021.

Su, H., Wei, Y., Lu, W., Yan, X.-H., and Zhang, H.: Unabated Global Ocean Warming Revealed by Ocean Heat Content from Remote Sensing Reconstruction, Remote Sens., 15, 566, https://doi.org/10.3390/rs15030566, 2023.

Tan, Z., Zhang, B., Wu, X., Dong, M., and Cheng, L.: Quality control for ocean observations: From present to future, Sci. China Earth Sci., 65, 215–233, https://doi.org/10.1007/s11430-021-9846-7, 2022.

https://doi.org/10.5194/essd-2026-106
Preprint. Discussion started: 26 February 2026
© Author(s) 2026. CC BY 4.0 License.

929 Tan, Z., Cheng, L., Gouretski, V., Zhang, B., Wang, Y., Li, F., Liu, Z., and Zhu, J.: A new automatic quality
930 control system for ocean profile observations and impact on ocean warming estimate, Deep Sea Res. Part
931 Oceanogr. Res. Pap., 194, 103961, https://doi.org/10.1016/j.dsr.2022.103961, 2023.

932 Thomson, R. E. and Emery, W. J.: Data Analysis Methods in Physical Oceanography, Newnes, 729 pp., 2014.

933 Venegas, R. M., Acevedo, J., and Treml, E. A.: Three decades of ocean warming impacts on marine ecosystems:
934 A review and perspective, Deep Sea Res. Part II Top. Stud. Oceanogr., 212, 105318,
935 https://doi.org/10.1016/j.dsr2.2023.105318, 2023.

936 Wild, M.: The global energy balance as represented in CMIP6 climate models, Clim. Dyn., 55, 553–577,
937 https://doi.org/10.1007/s00382-020-05282-7, 2020.

938 Wu, Q., Gregory, J. M., Zanna, L., and Khatiwala, S.: Time-varying global energy budget since 1880 from a
939 reconstruction of ocean warming, Proc. Natl. Acad. Sci., 122, e2408839122,
940 https://doi.org/10.1073/pnas.2408839122, 2025.

941 Zanna, L., Khatiwala, S., Gregory, J. M., Ison, J., and Heimbach, P.: Global reconstruction of historical ocean
942 heat storage and transport, Proc. Natl. Acad. Sci., 116, 1126–1131, https://doi.org/10.1073/pnas.1808838115,
943 2019.

944 Zhang, B., Cheng, L., Tan, Z., Gouretski, V., Li, F., Pan, Y., Yuan, H., Ren, H., Reseghetti, F., Zhu, J., and
945 Wang, F.: CODC-v1: a quality-controlled and bias-corrected ocean temperature profile database from 1940–
946 2023, Sci. Data, 11, 666, https://doi.org/10.1038/s41597-024-03494-8, 2024.

947 Zhang, C., Wang, D., Liu, Z., Lu, S., Sun, C., Wei, Y., and Zhang, M.: Global Gridded Argo Dataset Based on
948 Gradient-Dependent Optimal Interpolation, J. Mar. Sci. Eng., 10, 650, https://doi.org/10.3390/jmse10050650,
949 2022.